Table 3
Immunolocalization of Efp in human tissues

Tissues	Types of Efp positive cell			
	n	Adult	*n*	Fetal
Placenta	3	Cytotrophoblasts, decidual cell	0	NA
Uterus	3	Endometrial epithelial cell	2	Endometrial epithelial cell
Testis	3	Ductal cell, leydig cell	3	Ductal cell, mesenchymal cell
Prostate	2	Grandular epithelium	0	NA
Thyroid gland	3	Follicular epithelium	1	Follicular epithelium
Adrenal gland	5	None	2	None
Brain	0	NA	5	Nerve cell
Heart	2	None	2	None
Aorta and blood vessel	2	Endothelial cell	2	Endothelial cell
Trachea and bronchus	2	Epithelial cell	5	Epithelial cell
Lung	4	Alveolar epithelium	4	None
Thymus	2	Thymic epithelial cell	3	Thymic epithelial cell
Esophagus	2	Glandular epithelium	1	None
Stomach	2	None	3	None
Small and large intestine	3	Epithelial cell	4	Epithelial cell
Liver	2	Hepatocyte	3	Hepatocyte
Gall bladder	5	None	0	NA
Pancreas	2	Ductal epithelium	2	Ductal epithelium
Spleen	2	Splenic macrophage	2	None
Kidney	3	Epithelium of proximal tubule	2	Epithelium of proximal tubule
Urinary bladder	2	Transitional epithelium	3	Transitional epithelium
Cartilage	2	None	5	Chondrocyte
Salivary gland	2	Ductal epithelium	0	NA

NA: samples were not available; none: there was not significant immunoreactivity.

erally considered to play an important role in the regulation of placental function. ERα was expressed in cytotrophoblast cells, not in syncytiotrophoblast cells, and diminution of ERα and appearance of ERβ were demonstrated to be associated with the development of syncytiotrophoblast cells (Bukovsky et al., 2003a,b). Orimo et al. (1995) demonstrated that Efp was mainly expressed in female reproductive organs in mice, including uterus, ovary, and mammary gland, and was colocalized with ER. The study of Efp knockout mice subsequently revealed that Efp is essential for estrogen-induced cell proliferation as one of the direct targets of ERα (Orimo et al., 1999). Therefore, it is suggested that Efp is closely involved in the estrogenic actions, including the growth and/or differentiation, in these female reproductive organs through ERα.

High level of Efp mRNA expression was also detected in the aorta (endothelial cells) and spleen (splenic macrophages). Estrogen modulates vascular functions, and vascular endothelium is associated with expression of both ERα and ERβ (Suzuki et al., 2003). Estrogen reduces the vascular injury in wild-type, ERα knockout (ERαKO) (Sullivan et al., 1995; Iafrati et al., 1997), and ERβKO (Karas et al., 1999), but could not reduce the injury in ERαβ double KO mice (Karas et al., 2001). ERs were also detected in splenic macrophages (Kramer and Wray, 2002). Erlandsson et al. (2001) further demonstrated that deletion of ERα led to hypoplasia of spleen in their study using ERαKO, ERβKO, and ERαβ double KO mice. However the detailed estrogenic functions remain unclear in human aorta or spleen. Therefore the estrogenic actions in these tissues above may be partly through the Efp expression.

In our study, relatively low levels of Efp mRNA expression were detected in various tissues including those in which the expression of ERs has been reported. Among human tissues examined, Efp immunoreactivity was mainly detected in the epithelial cells. Previous studies demonstrated the widespread distribution of ERβ in various human tissues both in adult and fetus (Taylor and Al-Azzawi, 2000; Takeyama et al., 2001). ERβ immunoreactivity was strongly detected in the follicular epithelium of human thyroid gland

Fig. 2. Immunohistochemistry for Efp in human tissues. Efp immunoreactivity was detected in the endometrial epithelial cells in the uterus (A). No immunoreactivity was detected in the negative control using the serial section (B). In the lung, Efp immunoreactivity was detected in the alveolar epithelium (arrows) (C). Efp immunoreactivity was detected in follicular epithelium of the thyroid gland (arrows) (D). In the kidney, Efp immunoreactivity was detected in epithelium of the proximal tubule (arrows) (E). Glandular epithelial cells (arrows) were positive for Efp in the esophagus (F). In the placenta, Efp was positive in the cytotrophoblast (cy) but not syncytiotrophoblasts (sy) (G). In the spleen, Efp immunoreactivity was sporadically found in the marginal zone (H). These cells were also positive for CD68 (arrows) in the serial section (I), suggesting the splenic macrophages. Hematoxylin was used for counterstaining in (I). In fetal aorta, Efp immunoreactivity was detected in endothelial cells (arrows) (J). Efp immunoreactivity was detected in epithelium of the proximal tubule (arrows) in the fetal kidney (K). Efp was immunolocalized in the epithelium of the fetal colon (L): bar = 100 μm, respectively.

from 11 gestational weeks, suggesting the important estrogen actions in the development and/or maintenance of thyroid follicular functions through ERβ (Kawabata et al., 2003). ERβ was also reported in glandular epithelium of the prostate (Tsurusaki et al., 2003), epithelium of respiratory system (Taylor and Al-Azzawi, 2000), and epithelium of the stomach (Matsuyama et al., 2002) and colon (Konstantinopoulos et al., 2003), where Efp immunoreactivity was detected in our present immunohistochemical study. On the other hand, ERβ was also detected in interstitial cells such as adipocytes, smooth muscle cells and fibroblasts (Taylor and Al-Azzawi, 2000; Joyner et al., 2001; Haczynski et al., 2002), while Efp immunoreactivity was not detected in these cells in our present study. Therefore, Efp is considered to be involved in the regulation of estrogen related functions in epithelial cells in these tissues, possibly through ERβ, but not in that of stromal cells.

In summary, our present results demonstrated that Efp is widely expressed in human adult and fetal tissues. The Efp-positive cells were generally associated with the expression of ERα and/or ERβ previously, and therefore, it is suggested that Efp plays important roles in various human tissues possibly through ERs. Further examinations, including functional studies, are required to clarify these hypotheses or to understand the detailed biological significance of Efp in human tissues.

Acknowledgements

We thank Dr. F. Nagaike (Nagaike Maternal Clinic) and Dr. K. Kitamura (Department of Obstetrics and Gynecology, Tohoku University Hospital) for providing tissue samples. We appreciate the skillful technical assistance of Ms. Y. Murakami, Ms. C. Kaneko and Mr. K. Ono in the Department of Pathology, Tohoku University School of Medicine.

References

Albertazzi, P., Purdie, D.W., 2001. The life and times of the estrogen receptors: an interim report. Climacteric 4, 194–202.

Bukovsky, A., Cekanova, M., Caudle, M.R., Wimalasena, J., Foster, J.S., Henley, D.C., Elder, R.F., 2003a. Expression and localization of estrogen receptor-alpha protein in normal and abnormal term placentae and stimulation of trophoblast differentiation by estradiol. Reprod. Biol. Endocrinol. 1, 13.

Bukovsky, A., Caudle, M.R., Cekanova, M., Fernando, R.I., Wimalasena, J., Foster, J.S., Henley, D.C., Elder, R.F., 2003b. Placental expression of estrogen receptor beta and its hormone binding variant—comparison with estrogen receptor alpha and a role for estrogen receptors in asymmetric division and differentiation of estrogen-dependent cells. Reprod. Biol. Endocrinol. 1, 36.

Dickson, R.B., Stancel, G.M., 2000. Estrogen receptor-mediated processes in normal and cancer cells. J. Natl. Cancer Inst. Monogr. 27, 135–145.

Dumoulin, F.L., Nischalke, H.D., Leifeld, L., von dem Bussche, A., Rockstroh, J.K., Sauerbruch, T., Spengler, U., 2000. Semi-quantification of human C–C chemokine mRNAs with reverse transcription/real-time PCR using multi-specific standards. J. Immunol. Methods 241, 109–119.

Erlandsson, M.C., Ohlsson, C., Gustafsson, J.A., Carlsten, H., 2001. Role of oestrogen receptors alpha and beta in immune organ development and in oestrogen-mediated effects on thymus. Immunology 103, 17–25.

Haczynski, J., Tarkowski, R., Jarzabek, K., Slomczynska, M., Wolczynski, S., Magoffin, D.A., Jakowicki, J.A., Jakimiuk, A.J., 2002. Human cultured skin fibroblasts express estrogen receptor alpha and beta. Int. J. Mol. Med. 10, 149–153.

Iafrati, M.D., Karas, R.H., Aronovitz, M., Kim, S., Sullivan Jr., T.R., Lubahn, D.B., O'Donnell Jr., T.F., Korach, K.S., Mendelsohn, M.E., 1997. Estrogen inhibits the vascular injury response in estrogen receptor alpha-deficient mice. Nat. Med. 3, 545–548.

Ikeda, K., Orimo, A., Higashi, Y., Muramatsu, M., Inoue, S., 2000. Efp as a primary estrogen-responsive gene in human breast cancer. FEBS Lett. 472, 9–13.

Inoue, S., Orimo, A., Hosoi, T., Kondo, S., Toyoshima, H., Kondo, T., Ikegami, A., Ouchi, Y., Orimo, H., Muramatsu, M., 1993. Genomic binding-site cloning reveals an estrogen-responsive gene that encodes a RING finger protein. Proc. Natl. Acad. Sci. U.S.A. 90, 11117–11121.

Joyner, J.M., Hutley, L.J., Cameron, D.P., 2001. Estrogen receptors in human preadipocytes. Endocrine 15, 225–230.

Karas, R.H., Hodgin, J.B., Kwoun, M., Krege, J.H., Aronovitz, M., Mackey, W., Gustafsson, J.A., Korach, K.S., Smithies, O., Mendelsohn, M.E., 1999. Estrogen inhibits the vascular injury response in estrogen receptor beta-deficient female mice. Proc. Natl. Acad. Sci. U.S.A. 96, 15133–15136.

Karas, R.H., Schulten, H., Pare, G., Aronovitz, M.J., Ohlsson, C., Gustafsson, J.A., Mendelsohn, M.E., 2001. Effects of estrogen on the vascular injury response in estrogen receptor alpha, beta (double) knockout mice. Circ. Res. 89, 534–539.

Kawabata, W., Suzuki, T., Moriya, T., Fujimori, K., Naganuma, H., Inoue, S., Kinouchi, Y., Kameyama, K., Takami, H., Shimosegawa, T., Sasano, H., 2003. Estrogen receptors (alpha and beta) and 17beta-hydroxysteroid dehydrogenase type 1 and 2 in thyroid disorders: possible in situ estrogen synthesis and actions. Mod. Pathol. 16, 437–444.

Konstantinopoulos, P.A., Kominea, A., Vandoros, G., Sykiotis, G.P., Andricopoulos, P., Varakis, I., Sotiropoulou-Bonikou, G., Papavassiliou, A.G., 2003. Oestrogen receptor beta (ERbeta) is abundantly expressed in normal colonic mucosa, but declines in colon adenocarcinoma paralleling the tumour's dedifferentiation. Eur. J. Cancer 39, 1251–1258.

Kramer, P.R., Wray, S., 2002. 17-Beta-estradiol regulates expression of genes that function in macrophage activation and cholesterol homeostasis. J. Steroid. Biochem. Mol. Biol. 81, 203–216.

Kuiper, G.G., Enmark, E., Pelto-Huikko, M., Nilsson, S., Gustafsson, J.A., 1996. Cloning of a novel receptor expressed in rat prostate and ovary. Proc. Natl. Acad. Sci. U.S.A. 93, 5925–5930.

Matsuyama, S., Ohkura, Y., Eguchi, H., Kobayashi, Y., Akagi, K., Uchida, K., Nakachi, K., Gustafsson, J.A., Hayashi, S., 2002. Estrogen receptor beta is expressed in human stomach adenocarcinoma. J. Cancer Res. Clin. Oncol. 128, 319–324.

Mosselman, S., Polman, J., Dijkema, R., 1996. ER beta: identification and characterization of a novel human estrogen receptor. FEBS Lett. 392, 49–53.

Orimo, A., Inoue, S., Ikeda, K., Noji, S., Muramatsu, M., 1995. Molecular cloning, structure, and expression of mouse estrogen-responsive finger protein Efp. Co-localization with estrogen receptor mRNA in target organs. J. Biol. Chem. 270, 24406–24413.

Orimo, A., Inoue, S., Minowa, O., Tominaga, N., Tomioka, Y., Sato, M., Kuno, J., Hiroi, H., Shimizu, Y., Suzuki, M., Noda, T., Muramatsu, M., 1999. Underdeveloped uterus and reduced estrogen responsiveness in mice with disruption of the estrogen-responsive finger protein gene, which is a direct target of estrogen receptor alpha. Proc. Natl. Acad. Sci. U.S.A. 96, 12027–12032.

Saurin, A.J., Borden, K.L., Boddy, M.N., Freemont, P.S., 1996. Does this have a familiar RING? Trends Biochem. Sci. 21, 208–214.

Sullivan Jr., T.R., Karas, R.H., Aronovitz, M., Faller, G.T., Ziar, J.P., Smith, J.J., O'Donnell Jr., T.F., Mendelsohn, M.E., 1995. Estrogen inhibits the response-to-injury in a mouse carotid artery model. J. Clin. Invest. 96, 2482–2488.

Suzuki, T., Nakamura, Y., Moriya, T., Sasano, H., 2003. Effects of steroid hormones on vascular functions. Microsc. Res. Tech. 60, 76–84.

Takeyama, J., Suzuki, T., Inoue, S., Kaneko, C., Nagura, H., Harada, N., Sasano, H., 2001. Expression and cellular localization of estrogen receptors alpha and beta in human fetus. J. Clin. Endocrinol. Metab. 86, 2258–2262.

Taylor, A.H., Al-Azzawi, F., 2000. Immunolocalisation of oestrogen receptor beta in human tissues. J. Mol. Endocrinol. 24, 145–155.

Thomson, S.D., Ali, S., Pickles, L., Taylor, J., Pace, P.E., Lymboura, M., Shousha, S., Coombes, R.C., 2001. Analysis of estrogen-responsive finger protein expression in benign and malignant human breast. Int. J. Cancer 91, 152–158.

Tokunaga, K., Nakamura, Y., Sakata, K., Fujimori, K., Ohkubo, M., Sawada, K., Sakiyama, S., 1987. Enhanced expression of a glyceraldehyde-3-phosphate dehydrogenase gene in human lung cancers. Cancer Res. 47, 5616–5619.

Tsai, M.J., O'Malley, B.W., 1994. Molecular mechanisms of action of steroid/thyroid receptor superfamily members. Ann. Rev. Biochem. 63, 451–486.

Tsurusaki, T., Aoki, D., Kanetake, H., Inoue, S., Muramatsu, M., Hishikawa, Y., Koji, T., 2003. Zone-dependent expression of estrogen receptors alpha and beta in human benign prostatic hyperplasia. J. Clin. Endocrinol. Metab. 88, 1333–1340.

Urano, T., Saito, T., Tsukui, T., Fujita, M., Hosoi, T., Muramatsu, M., Ouchi, Y., Inoue, S., 2002. Efp targets 14-3-3σ for proteolysis and promotes breast tumour growth. Nature 417, 871–875.

Decreased Expression of 14-3-3σ Is Associated with Advanced Disease in Human Epithelial Ovarian Cancer: Its Correlation with Aberrant DNA Methylation

Jun-ichi Akahira,[1,2] Youko Sugihashi,[1] Takashi Suzuki,[2] Kiyoshi Ito,[1] Hitoshi Niikura,[1] Takuya Moriya,[2] Makoto Nitta,[3] Hitoshi Okamura,[3] Satoshi Inoue,[4] Hironobu Sasano,[2] Kunihiro Okamura,[1] and Nobuo Yaegashi[1]

Departments of [1]Obstetrics and Gynecology, and [2]Pathology, Tohoku University Graduate School of Medicine, Sendai, Japan; [3]Department of Obstetrics and Gynecology, Kumamoto University School of Medicine, Kumamoto, Japan; and [4]Division of Gene Regulation and Signal Transduction, Research Center for Genomic Medicine, Saitama Medical School, Saitama, Japan

ABSTRACT

Purpose: **In this study, we examined the promoter methylation status and expression of 14-3-3σ and evaluated its clinical significance in epithelial ovarian cancer.**

Experimental Design: **Twelve ovarian cancer cell lines; 2 ovarian surface epithelial cell lines; and 8 normal, 8 benign, 12 borderline, and 102 ovarian cancer tissues were examined. Methylation-specific PCR, quantitative reverse transcription-PCR, and immunohistochemistry were used to evaluate methylation status and expression of *14-3-3σ* gene and protein.**

Results: **Among the 12 ovarian cancer cell lines, the presence of a methylated band was detected in seven cell lines. Median values of relative *14-3-3σ* gene expression in cancers with methylation (3.27) were significantly lower than those without methylation (16.4; $P < 0.001$). Treatment of 5-aza-2′-deoxycitidine resulted in the demethylation of the promoter CpG islands and reexpression. All of the normal, benign, and borderline tissues were positive for 14-3-3σ protein, and in ovarian cancer tissues, 73.5% (75 of 102) were positive for 14-3-3σ protein and was almost consistent with methylation status. Negative immunoreactivity of 14-3-3σ was significantly correlated with high age and serous histology, high-grade, advanced-stage residual tumor of >2 cm, high serum CA125, high Ki-67 labeling index, and positive p53 immunoreactivity. 14-3-3σ immunoreactivity was significantly associated with overall survival ($P = 0.0058$).**

Conclusions: **Our findings suggest that 14-3-3σ is inactivated mainly by aberrant DNA methylation and that it may play an important role in the pathogenesis of epithelial ovarian cancer.**

INTRODUCTION

Epithelial ovarian cancer is the leading cause of death from gynecological malignancies in the great majority of developed countries (1). This high mortality is considered to be, in large part, due to the advanced stage of the disease commonly present at the time of diagnosis, but many clinical studies have reported that there are some prognostic factors in ovarian cancer other than clinical stages, such as histology, the degree of primary surgical cytoreduction, and response to chemotherapy (1–3). Other prognostic parameters have been also proposed in addition to those relatively established parameters. These include Ki67 index, progesterone receptor, and the preoperative serum maker CA125, and others (4–6). The identification of new prognostic factors may further contribute to improve treatment and clinical outcome of ovarian cancer patients.

The cause of epithelial ovarian cancer is still unknown. Although *BRCA1* and *BRCA2* mutation have been identified as associated with susceptibility to ovarian cancer (7, 8), mutations in these genes account for only 2–3% of all ovarian cancers. The remaining cases are considered to be sporadic in nature and arise as a result of acquired alterations in oncogenes and tumor suppressor genes such as *TP53* and *PTEN* (9–11).

DNA methylation has an essential regulatory function in mammalian development, suppressing gene activity by changing chromatin structure (12, 13). It has become apparent that aberrant DNA methylation of promoter region CpG islands may serve as an alternate mechanism to genetic defects in the inactivation of tumor suppressor genes in human cancers (14, 15). Accordingly, the identification of gene targets of methylation-associated silencing could lead to novel genes involved in the initiation and progression of human neoplasia.

14-3-3σ was originally identified as a p53-inducible gene that is responsive to DNA damaging agents (16). Recent study demonstrated that 14-3-3σ protein plays a crucial role in the G_2 checkpoint by sequestering the mitotic initiation complex, cdc2-cyclin B1, in the cytoplasm after DNA damage (17). This prevents cdc2-cyclin B1 from entering the nucleus in which the protein complex would normally initiate mitosis. In this manner, 14-3-3σ induces G_2 arrest and allows the repair of damaged DNA (16, 17). The expression of 14-3-3σ is reported to be frequently lost in human breast, gastric, and lung cancers, and the inactivation is due to

Received 10/31/03; revised 12/3/03; accepted 12/19/03.
Grant support: Supported in part by a grant-in-aid for Scientific Research from the Ministry of Health and Welfare, a grant-in-aid from the Ministry of Education, Science and Culture, a grant-in-aid from Kurokawa Cancer Research Foundation, and a grant-in-aid from Japan Society of Gynecologic Oncology (JSGO).
The costs of publication of this article were defrayed in part by the payment of page charges. This article must therefore be hereby marked *advertisement* in accordance with 18 U.S.C. Section 1734 solely to indicate this fact.
Requests for reprints: Jun-ichi Akahira, Department of Obstetrics and Gynecology, Tohoku University Graduate School of Medicine, 1-1 Seiryo-machi, Aoba-ku, Sendai, 980-8574, Japan. Phone: 81-22-717-7254; Fax: 81-22-717-7258; E-mail: jakahira-tohoku@umin.ac.jp.

aberrant DNA methylation (18–20). However, the expression of 14-3-3σ and its mechanism have not been examined in epithelial ovarian cancer. Therefore, in this study, we examined the promoter methylation status and expression of 14-3-3σ in epithelial ovarian cancer cells. We also evaluated the correlation between 14-3-3σ expression and clinicopathological parameters in patients with epithelial ovarian cancer.

MATERIALS AND METHODS

Tissues and Cells. Eight normal ovaries, 8 ovarian serous cystadenomas, 12 serous borderline tumors, and 102 ovarian cancer cases were obtained from patients after surgical therapy from 1988 to 2000 at Tohoku University Hospital, Sendai, Japan. In ovarian cancer patients, information regarding age, performance status on admission, histology, stage, grade, residual tumor after primary surgery, and overall survival were retrieved from the review of patient charts. Median follow-up time of the patients in this study was 59 months (4–120 months). Eighty-four (82.3%) of 102 patients received platinum-containing chemotherapy after operation. Patients who have early-stage (stage Ia) and low grade-disease (G1, G2) and patients who have poor performance status did not receive platinum-based chemotherapy. Performance status was defined according to WHO criteria (21). Histology and stage were determined according to FIGO (International Federation of Gynecology and Obstetrics) criteria. Grade was evaluated by one of the authors (T. M.) using universal grading system in epithelial ovarian cancer (22). Residual disease was determined by the amount of unresectable tumor that remained after primary cytoreductive surgery. Optimal cytoreduction was defined as no gross residual tumor greater than 2 cm in diameter, and suboptimal cytoreduction was defined as any gross residual disease remaining greater than 2 cm in diameter. Overall survival was calculated from the time of initial surgery to death, or the date of last contact. Survival times of patients still alive or lost to follow-up were censored in December 2002. All of these archival specimens were retrieved from the surgical pathology files at Tohoku University Hospital, Sendai, Japan. These specimens were all fixed in 10% formalin and embedded in paraffin. The research protocol was approved by the ethics committee of Tohoku University Graduate School of Medicine.

OVCAR3, Caov3, SKOV3, TOV112D, TOV21G, OV90, and ES2 (adenocarcinoma, OVCAR3, SKOV3; serous adenocarcinoma, Caov3, OV90; clear cell adenocarcinoma, TOV21G, ES2; endometrioid adenocarcinoma, TOV112D) cell lines were purchased from American Type Culture Collection. JHOS2, JHOS3, HTOA, OMC3, and JHOC5 (serous adenocarcinoma, JHOS2, JHOS3, HTOA; mucinous adenocarcinoma, OMC3; clear cell adenocarcinoma, JHOC5) cell lines were purchased from Riken cell bank (Tsukuba, Japan). Normal ovarian surface epithelial cell lines (OSE2 and OSE4) were established by one of the authors (M. N.; Ref. 23). Cell lines were maintained in DMEM/F12 (Invitrogen) supplemented with 10% fetal bovine serum and 1% penicillin/streptomycin (Invitrogen), and were incubated in 5% CO_2 at 37°C. For 5-aza-2′ deoxycytidine (5azaC) treatment, 1×10^6 cells were seeded into T75 flasks and were treated with 0.5 μM or 1.0 μM 5azaC (Sigma) for 72 h.

Methylation-Specific PCR. Methylation status of the samples was investigated by methylation-specific PCR as described in the literature (24). Genomic DNA of ovarian cancer tissue was extracted using a laser capture microdissection and treated with proteinase K (0.5 mg/ml) for 48 h at 37°C. Genomic DNA from ovarian cancer cell lines was extracted using AquaPure Genomic DNA kit (Bio-Rad). The quality and integrity of the DNA was determined by the A260:280 ratio. One μg of genomic DNA was treated with sodium bisulfite using CpGenome DNA modification kit (Intergen) according to the instructions. Amplification was achieved in a 20-μl reaction volume containing 2 μl of 10× Ex Taq Buffer, 1.5 μl of 25 mM $MgCl_2$, 1 μM each primer, 1.5 μl of 2.5 mM dNTPs, and 1 unit of Takara Ex Taq polymerase (Takara, Japan). Hot-start PCR was performed in a thermal cycler (Takara) for 35 cycles, each of which consisted of denaturation at 96°C for 30 s, annealing at 64°C for 30 s, and extension at 72°C for 90 s, followed by a final 10 min extension at 72°C. Primers used were 5′-TGGTAGTTTTTATGAAAGGCGTC-3′ and 5′-CCTCTAACCGCCCACCACG-3′ (104-bp) for the methylated reaction (M primers), and 5′-ATGGTAGTTTTTATGAAAGGTGTT-3′ and 5′-CCCTCTAACCACCCACCACA-3′ (106-bp) for the unmethylated reaction (U primers; Ref. 18). Universal methylated human male genomic DNA (Intergen) was used as a positive control for methylated reaction. Genomic DNA purified from MCF-7 breast cancer cell line was used as a positive control for unmethylated reaction (18). A blank control containing all of the PCR components except template DNA was also included in all of the PCRs. Reaction products were separated by electrophoresis on a 3% agarose gel, stained with ethidium bromide, and visualized under UV illumination. Specimens with purely unmethylated promoters have positive PCR products by U primers but not with the M primers. Specimens that contain purely methylated promoters will have PCR products by using M primers but not with the U primers. Specimens that contain heterogeneous status of both methylated and unmethylated promoters have PCR products from both U primers and M primers.

Reverse Transcription and Real-Time Quantitative PCR. Total RNA was isolated from cell lines by phenol-chloroform extraction using Isogen (Nippon Gene, Tokyo, Japan). RNA was treated with RNase-free DNase (Roche Diagnostics; 1 μg/μl) for 2 h at 37°C, followed by heat inactivation at 65°C for 10 min. A reverse transcription-PCR kit (SUPERSCRIPT II First-strand synthesis system, Invitrogen) was used and cDNA synthesis was carried out according to the instructions. cDNAs were synthesized from 2 μg of total RNA using random hexamer, and reverse transcription was carried out for 50 min at 42°C with SUPERSCRIPT II reverse transcriptase. Real-time quantitative PCR was performed using the iCycler system (Bio-Rad). For the determination of 14-3-3σ cDNA content, a 25-μl reaction mixture consisted of 23 μl iQ SYBR Green MasterMix, 1 μM each primer, and 1 μl of template cDNA were prepared. The PCR conditions were as follows: initial duration at 96°C for 60 s, and followed by 35 cycles with denaturation at 96°C for 30 s, annealing at 64°C (both for 14-3-3σ and β-actin) for 30 s, and extension at 72°C for 30 s. The fluorescence intensity of the double-strand specific SYBR Green I, reflecting the amount of formed PCR-product, was read at 88°C after the end of each elongation step. Primers used were

as follows: 14-3-3σ, 5′-CCTGCTGGACAGCCACCTCA-3′ and 5′-TGTCGGCCGTCCACAGTGTC-3′ (397-bp; Ref. 20); β-actin, 5′-CCAACCGCGAGAAGATGA-3′ and 5′-GGAAGGAAGGCTGGAAGAGT-3′ (459-bp; Ref. 25). β-actin cDNA fragments were amplified as internal positive controls. Normal human ovarian cDNA library (Stratagene, La Jolla, CA) was used as a normal control, cDNA from MCF-7 was used as a positive control, and water blank was used as a negative PCR control (data not shown). Control reactions in which reverse transcriptase was omitted were amplified under the same conditions to exclude DNA contamination (data not shown). Two independent quantitative PCR reactions were performed for each sample.

Immunohistochemistry. Immunohistochemical analysis was performed using the streptavidin-biotin amplification method using a Histofine kit (Nichirei, Tokyo, Japan), and have been previously described in detail (26). Polyclonal antibody for 14-3-3σ (N-14), monoclonal antibody for p53 (B20.1), and monoclonal antibody for Ki-67 (MIB-1) were purchased from Santa Cruz Biotechnology, Inc. (Santa Cruz, CA), Biomeda (Foster City, CA), and DAKO (Tokyo, Japan), respectively.

For antigen retrieval, the slides were heated in an autoclave at 120°C for 5 min in citric acid buffer [2 mM citric acid and 9 mM trisodium citrate dyhydrate (pH 6.0)]. The dilutions of primary antibodies for 14-3-3σ, p53 and Ki-67 were 1:100, 1:40, and 1:300, respectively. The antigen-antibody complex was visualized with 3,3′-diaminobenzidine (DAB) solution [1 mM DAB, 50 mM Tris-HCl buffer (pH 7.6), and 0.006% H_2O_2], and counterstained with hematoxylin. Nonneoplastic breast epithelial tissue was used as a positive control (18). As negative controls, 0.01 M PBS and normal mouse IgG were used in place of primary antibodies.

The immunohistochemical expression of 14-3-3σ, p53, and Ki-67 was independently reviewed by two of the authors (J. A. and T. M.) who had no knowledge of the clinicopathological data. As immunoreactivities of 14-3-3σ and p53 were relatively homogeneous and clearly distinguished for positive and negative, they were classified into two groups: +, positive carcinoma cells; and −, no immunoreactivity. Scoring of Ki-67 in carcinoma cells was counted independently by these same two authors, and the percentage of immunoreactivity in at least 500 carcinoma cells, *i.e.*, labeling index, was determined. Whenever a difference of greater than 5% was observed between the two readings, slides were reviewed jointly, and a consensus was reached.

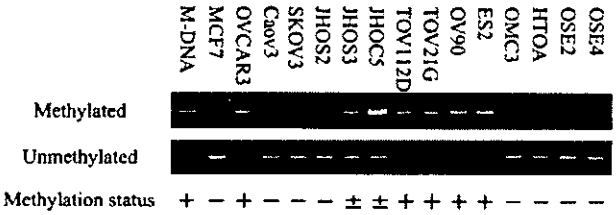

Fig. 1 Methylation-specific PCR (MSP) for 14-3-3σ in ovarian cancer and surface epithelial cell lines. Specimens with methylated promoters have positive PCR products in the *Methylated Lane*, and specimens with unmethylated promoters have positive PCR products in the *Unmethylated Lane*. Specimens that contain heterogeneous status of both methylated and unmethylated promoters have PCR products in both the *Methylated* and the *Unmethylated Lanes*. Methylation statuses of each cell line are defined as; +, purely methylated: −, purely unmethylated: ±, both methylated and unmethylated, and are shown in the *Methylation status Lane*. *M-DNA* (universal methylated human male genomic DNA) was used as a positive control for methylated reaction. MCF-7 (*MCF7*) breast cancer cell line was used as a positive control for unmethylated reaction.

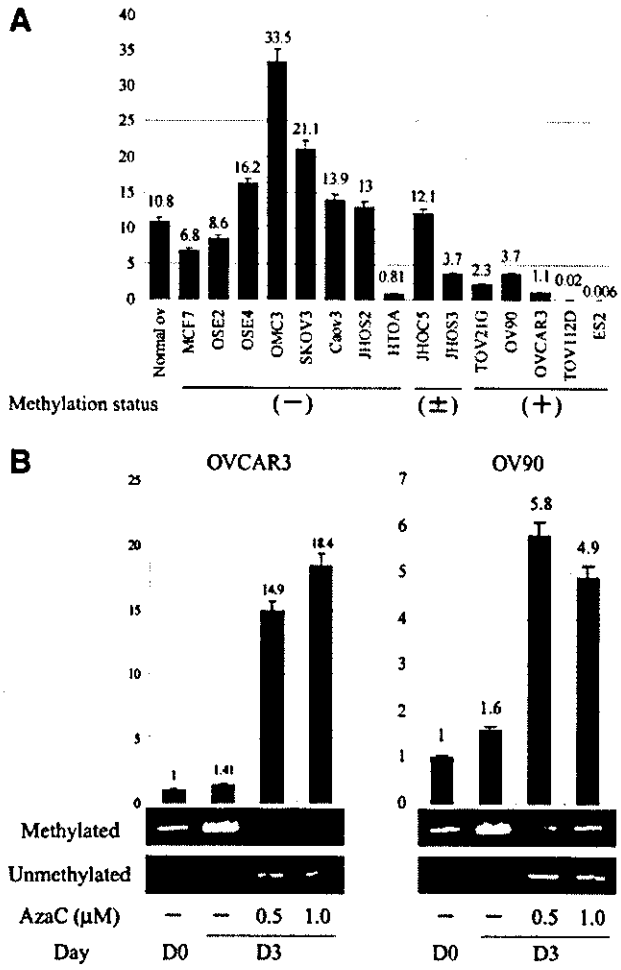

Fig. 2 *A*, expression of the *14-3-3σ* gene in ovarian cancer cells. Mean of the two independent results of real-time quantitative reverse transcription (RT)-PCR of ovarian cancer and surface epithelial cell lines are shown. *The number on top of each bar*, relative *14-3-3σ* gene expression standardized by the amount of internal positive control (β-actin). Normal ov (normal human ovarian cDNA library) was used as a normal control. MCF-7 was used as a positive control. *B*, reexpression of the *14-3-3σ* gene by 5-aza-2′-deoxycitidine (5azaC) treatment. OVCAR3 and OV90 cell lines that have only methylated bands were treated with 5azaC for 3 days. Methylation status and mRNA expression of 14-3-3σ was assessed by methylation-specific PCR (MSP) and quantitative RT-PCR on day 0 (*D0*) and day 3 (*D3*) with or without 5azaC (0.5 μM and 1.0 μM) treatment (*AzaC*). Complete and partial demethylation was observed in OVCAR3 and OV90, respectively. *The number on the top of each bar*, relative *14-3-3σ* gene expression standardized by the amount of internal positive control (β-actin).

Statistical Analysis. Statistical analysis was performed using Stat View 5.0 (SAS Institute Inc.) software. The statistical significance between 14-3-3σ and characteristics of the patients was evaluated using Mann-Whitney *U* test, Kruskal-Wallis test, and Scheffe analysis. Correlation between 14-3-3σ and Ki-67, p53 immunoreactivity was also assessed using Mann-Whitney

U test. Univariate analysis of prognostic significance for prognostic factors was performed using a log-rank test, after each survival curve was obtained by the Kaplan-Meier method. Multivariate analysis was performed using Cox regression model to evaluate the predictive power of each variable independently of the others. All of the patients who could be assessed were included in the intention-to-treat analysis. A result was considered significant when the P was less than 0.05.

RESULTS

Methylation Status and Expression of 14-3-3σ in Ovarian Cancer Cells. Among the 12 ovarian cancer cell lines in which 14-3-3σ promoter methylation was investigated, the presence of a methylated band was detected in 7 cell lines, 2 of which were together with unmethylated band as shown in Fig. 1. The methylated band was detected in all of the cell lines derived from clear cell adenocarcinoma (TOV21G, ES2, JHOC5), two of five of serous adenocarcinoma (Caov3, OV90, JHOS2, JHOS3, HTOA), one of one of endometrioid adenocarcinoma (TOV112D), and none of one of mucinous adenocarcinoma (OMC-3). Both of the OSE cells were negative for methylated band.

The expression of *14-3-3σ* gene is shown in Fig. 2*A*. Quantitative reverse transcription-PCR was performed and the ratio of 14-3-3σ:β-actin was calculated to allow for comparison between the cell lines. Median values of relative *14-3-3σ* gene expression in cancers with methylation (3.27) were significantly lower than those without methylation (16.4; $P < 0.001$, Kruskal-Wallis test). In HTOA, the expression of *14-3-3σ* gene was relatively decreased, although this cell line did not have methylated promoter alleles. The expression of *14-3-3σ* gene was relatively high in OSE2 (8.6), OSE4 (16.2), and in the normal ovarian cDNA library (10.8).

To further confirm that aberrant DNA methylation contributed to loss of expression of *14-3-3σ* gene, we assessed the effect of 5azaC, a demethylating agent, on 14-3-3σ mRNA expression by quantitative reverse transcription-PCR. Treatment of OVCAR3 and OV90 cells with 5azaC for 3 days resulted in the complete and partial demethylation of the promoter CpG islands and reexpression of *14-3-3σ* gene, respectively (Fig. 2*B*). The amount of expression of mRNA after treatment (14.9 and 5.8 for 0.5 μM, and 18.4 and 4.9 for 1.0 μM in OVCAR and OV90, respectively) was significantly higher than that before

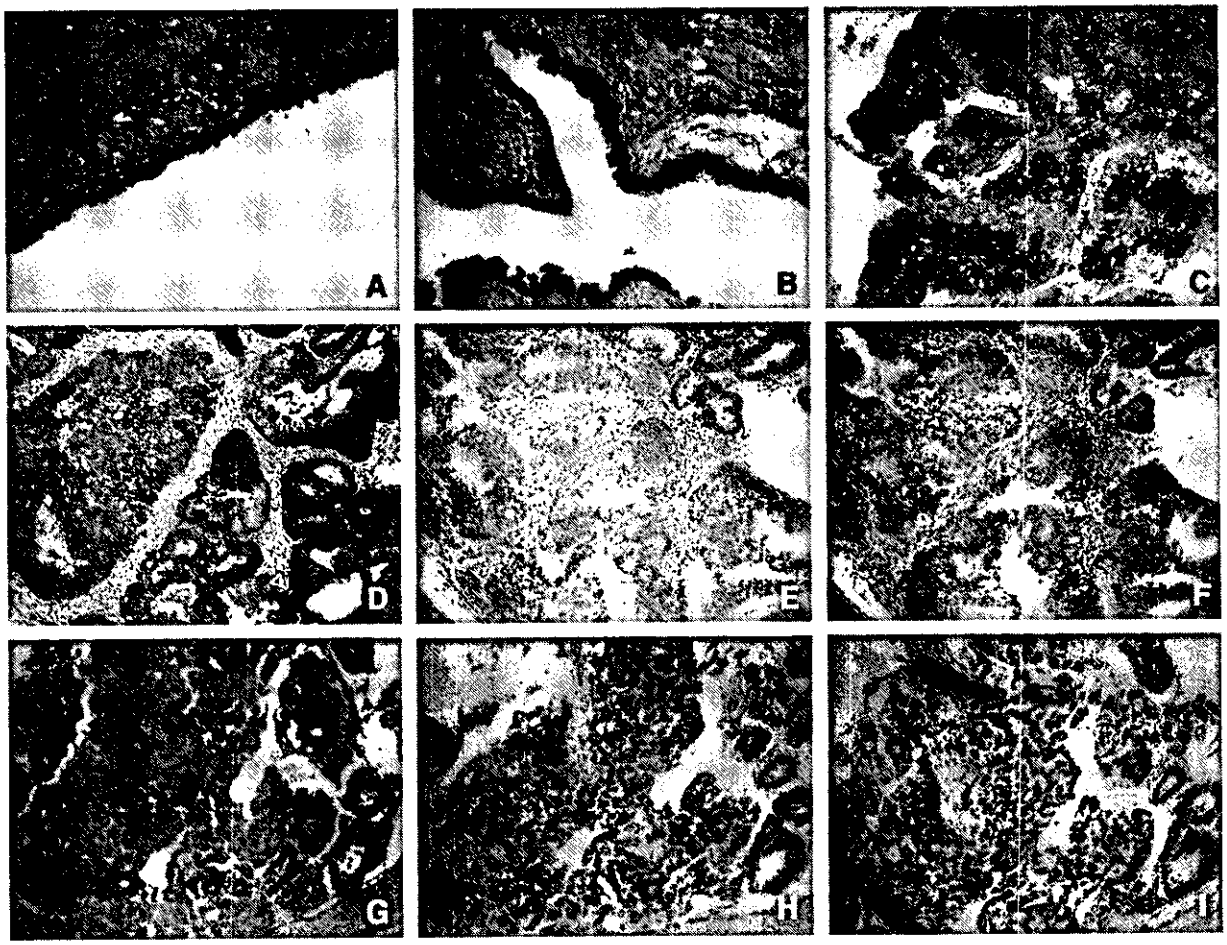

Fig. 3 Immunohistochemistry for 14-3-3σ in normal ovary, and in benign, borderline, and malignant ovarian tumors. Representative cases of immunohistochemistry for 14-3-3σ in the ovarian surface epithelium (*A*), benign adenoma (*B*), borderline tumor (*C*), two cases of epithelial ovarian cancer (*D, G*), and serial sections of each case for Ki-67 (*E, H*) and p53 (*F, I*) are shown. Note that positive 14-3-3σ case (*D*) is negative for Ki-67 (*E*) and p53 (*F*), whereas negative 14-3-3σ case (*G*) is positive for Ki-67 (*H*) and p53 (*I*). ×200 for all figures.

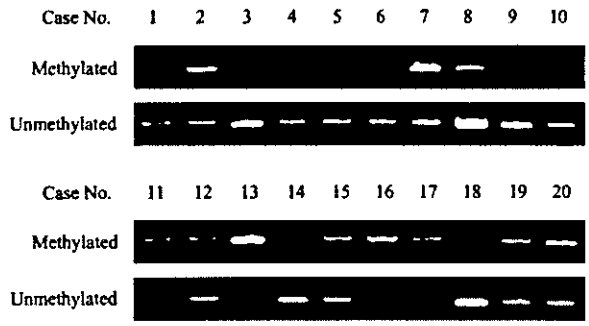

Fig. 4 Methylation-specific PCR (MSP) for *14-3-3σ* gene in ovarian cancer tissues. The methylation status of *14-3-3σ* gene in microdissected ovarian cancer tissues was evaluated by MSP in the 10 cases of positive (*Lanes 1–10*), and 10 cases of negative (*Lanes11–20*) immunoreactivity. Definition of *Methylated* and *Unmethylated Lanes* are the same as in Fig. 1.

treatment ($P < 0.001$, Kruskal-Wallis test). The decreased expression of 14-3-3σ in this cell line is, therefore, not attributable to abnormalities at the gene level or to the inability to express 14-3-3σ, but rather is directly related to the methylation.

Immunohistochemistry and Methylation Status of 14-3-3σ in Ovarian Cancer Tissues. Positive immunoreactivity for 14-3-3σ was detected in the cytoplasm of epithelial cells, although p53 and Ki-67 were confined exclusively to the nuclei of epithelial cells (Fig. 3). In normal, benign, and borderline tissues, all of the cases were positive for 14-3-3σ immunoreactivity. In ovarian cancer tissues, 73.5% (75 of 102) and 36.3% (37 of 102) were positive for 14-3-3σ and p53, respectively. Median Ki-67 labeling index was 17.2%.

To further clarify the relationships between 14-3-3σ immunoreactivity and aberrant DNA methylation in ovarian cancer tissues, we analyzed the methylation status in microdissected ovarian cancer tissues (Fig. 4). In the 10 cases of positive immunoreactivity, unmethylated bands were detected in all of the cases, and methylated bands were detected in 3 cases. In the another 10 cases of negative immunoreactivity, methylated bands were detected in 8 cases, although only unmethylated bands were detected in 2 cases.

Correlation between Clinicopathological Parameters and Immunohistochemistry in Ovarian Cancer Patients. Results of immunohistochemistry for 14-3-3σ, p53, and Ki-67 and correlation with clinicopathological parameters are summarized in Table 1. Negativity of 14-3-3σ was significantly correlated with high age, serous histology, high-grade, advanced-stage, residual tumor of >2 cm, high serum CA125, and high Ki-67 labeling index. Interestingly, p53 expression was inversely correlated with that of 14-3-3σ.

Results of univariate analysis of prognostic significance for

Table 1 Correlation between 14-3-3 σ immunoreactivity and clinicopathological parameters in epithelial ovarian cancer

			14-3-3 σ immunoreactivity		
	Total (n = 102)	%	+ (n = 75)	− (n = 27)	P
Age (median)	51		48.3	60.4	0.039
≦50	50	49.0	41	9	
>50	52	51.0	34	18	
Performance status[a]					
0–1	72	70.6	56	16	0.13
2–4	30	29.4	19	11	
Histology					
Serous	45	44.1	24	21	0.0003
Endometrioid	16	15.7	14	2	
Mucinous	14	13.7	14	0	
Clear cell	27	26.5	23	4	
Grade					
1	43	42.2	39	4	0.0022
2	35	34.3	23	12	
3	24	23.5	13	11	
Stage					
I/II	48	47.1	45	3	0.0001
III/IV	54	52.9	30	24	
Residual tumor[b]					
≤2 cm	62	60.8	55	7	0.0001
>2 cm	40	39.2	20	20	
CA125 (median, IU/liter)	255		43.5	63.9	0.0016
p53 immunoreactivity					
Positive	37	36.3	21	16	0.0038
Negative	65	63.7	54	11	
Ki67 LI (median)	17.2		15.6	24.4	0.047

[a] Performance status score: 0, asymptomatic and fully active; 1, symptomatic, fully ambulatory, restricted in physically strenuous activity; 2, symptomatic, ambulatory, capable of self-care, more than 50% of waking hours are spent out of bed; 3, symptomatic, limited self-care, spends more than 50% of time in bed, but not bedridden; 4, completely disabled, no self-care, bedridden.

[b] Residual tumor is defined in the "Materials and Methods."

[c] LI, labeling index.

Table 2 Univariate analysis of overall survival in epithelial ovarian cancer

Variable	*P*
14-3-3 σ (positive *vs.* negative)	0.0058
Age (≦50, >50)	0.029
PS[a] (0–1 *vs.* 2–4)	<0.0001
Histological type	0.913
Histological grade	0.05
Stage (I/II *vs.* III/IV)	<0.0001
Residual tumor (≤2 cm *vs.* >2 cm)	<0.0001
p53 (positive *vs.* negative)	0.36
Ki67 (<15% *vs.* >15%)	0.011

[a] PS, performance status.

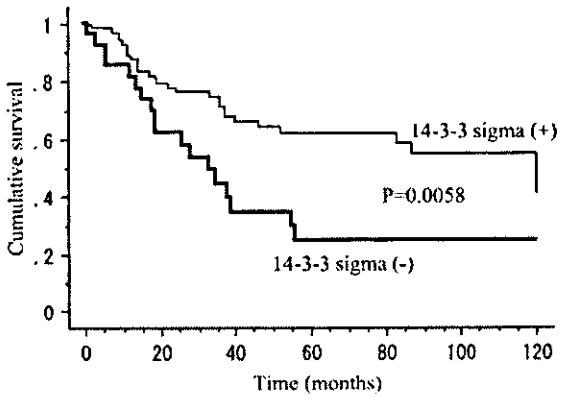

Fig. 5 Correlation between 14-3-3σ expression and overall survival in patients with epithelial ovarian cancer.

each variable with respect to survival are summarized in Table 2. In this analysis, we determined the positive cases of Ki-67 as those with a labeling index of more than 15%. Among the clinicopathological factors examined, those significantly associated with overall survival were 14-3-3σ immunoreactivity, age, performance status, grade, stage, residual tumor, and Ki-67. Negative 14-3-3σ cases had significantly worse overall survival rates than positive cases (Fig. 5; $P = 0.0058$). In multivariate analysis, 14-3-3σ immunoreactivity turned out not to be an independent prognostic indicator (Table 3). Among the variables examined, only stage and residual tumor turned out to be independent prognostic factors.

DISCUSSION

The aberrant methylation of 14-3-3σ was associated with loss of RNA expression, and the expression was restored by treatment with the demethylating agent 5azaC, indicating that aberrant DNA methylation is the main pathway of transcriptional silencing of *14-3-3σ* gene in ovarian cancer cells. Also, decreased expression of 14-3-3σ occurs in substantial proportion, and it turned out to be a prognostic factor in univariate analysis in epithelial ovarian cancer tissues. These results suggest the importance of the *14-3-3σ* gene in the development and progression of this tumor. To our knowledge, this is the first report on epigenetic silencing of 14-3-3σ in human ovarian cancer.

The *14-3-3σ* gene is demonstrated to be induced after DNA damage in a p53-dependent manner (16), and to play a role in the G_2 checkpoint by sequestering the Cdc2/cyclin B1 complex (17). Similar to our results, several authors demonstrated epigenetic inactivation of the *14-3-3σ* gene in human cancers (18, 20, 27). Experimental inactivation of the *14-3-3σ* gene causes a G_2 checkpoint defect, and results in the accumulation of chromosomal aberrations that increase the sensitivity to the DNA-damaging events (28, 29). In this context, it is of interest that serous histology in which significantly decreased expression of 14-3-3σ protein was observed is highly sensitive to chemotherapeutic agents. The histological type-specific expression of the *14-3-3σ* gene suggests that serous adenocarcinomas develop unique differentiation, different from other histological subtypes. Although a high proportion of human cancers are likely to have a chromosomal instability phenotype, mutations of the genes involving the G_2-M-phase checkpoint have rarely been found, and the mechanism of chromosomal instability in most of them is still unknown. Further study on the correlation between genetic instability and 14-3-3σ is needed.

In a number of previous reports, it is strongly postulated that the inactivation of 14-3-3σ might play an important role in tumor progression. Ostergaard *et al.* (30) showed that less-differentiated bladder squamous cell carcinoma is characterized by decreased expression of some proteins, including 14-3-3σ. Suzuki *et al.* (19) reported that aberrant methylation of the *14-3-3σ* gene was frequently observed in poorly differentiated gastric adenocarcinoma. Umbricht *et al.* (31) reported that decreased expression of 14-3-3σ was observed in 24 (96%) of 25 carcinomas, 15 (83%) of 18 of ductal carcinoma *in situ*, and 3 (38%) of 8 of atypical hyperplasias, and concluded that inactivation of 14-3-3-sigma occurs at an early stage in the progression of invasive breast cancer. Osada *et al.* (20) recently demonstrated frequent and type-specific inactivation of the *14-3-3σ* gene in small cell lung cancer. In our study, loss of 14-3-3σ expression was significantly correlated with high-grade advanced-stage bulky residual tumor and high serum CA125 and high Ki-67 levels, all of these factors represent fundamental difference in pathogenesis in ovarian cancer. Our results, together with previous reports, suggest that the loss of 14-3-3σ expression in ovarian cancer may have invasive and progressive characteristics.

Recent study suggests that promoter methylation increases with age in several genes in normal tissues, although the mechanism of age-related methylation is unknown (32, 33). Several factors may modulate age-related methylation, such as exogenous carcinogens, endogenously generated reactive oxygen species, and genetic differences in individual susceptibility (33). In our study, 14-3-3σ protein expression was decreased in elderly

Table 3 Multivariate analysis of overall survival using Cox's proportional hazard model

Variable	*P*
14-3-3 σ (positive *vs.* negative)	0.34
Age (≦50, >50)	0.15
PS[a] (0–1 *vs.* 2–4)	0.29
Histological grade	0.73
Stage (I/II *vs.* III/IV)	0.0081
Residual tumor (≤2 cm *vs.* >2 cm)	0.023
Ki67 (<15% *vs.* >15%)	0.11

[a] PS, performance status.

patients by immunohistochemistry. Although age-related methylation of *14-3-3σ* has not been reported, it is possible that expression of this gene is suppressed by methylation with age, and it may contribute to carcinogenesis in ovarian cancer.

In the present study, a clear correlation between aberrant methylation and silencing of 14-3-3σ was observed except for one cell line (HTOA) and 2 of 10 primary ovarian cancer tissues, which showed unmethylated patterns despite loss of 14-3-3σ expression. These results suggest that DNA methylation-independent mechanism may also be involved in the loss of 14-3-3σ expression. Several other ways of gene inactivation such as loss of transcription factor are assumed, and Osada *et al.* (20) considered that *14-3-3σ* gene silencing might occur without methylation in only primary tissues. From our results, positive p53 immunoreactivity, which suggests loss of functional p53 protein (34, 35), seems to contribute to the loss of 14-3-3σ expression in primary ovarian tissues. Possible methylation-independent mechanism remains to be elucidated to better understand the regulation of 14-3-3σ expression.

In conclusion, aberrant CpG island methylation is an epigenetic change that is largely responsible for silencing of the *14-3-3σ* gene. Inactivation of 14-3-3σ occurs in substantial proportion and may play a role as a potential tumor suppressor gene in epithelial ovarian cancer.

REFERENCES

1. Akahira J, Yoshikawa H, Shimizu Y, et al.Prognostic factors of stage IV epithelial ovarian cancer: a multicenter retrospective study. Gynecol Oncol 2001;81:398–403.

2. Del Campo JM, Felip E, Rubio D, et al. Long-term survival in advanced ovarian cancer after cytoreduction and chemotherapy treatment. Gynecol Oncol 1994;53:27–32.

3. Omura GA, Brady MF, Homesley HD, et al. Long-term follow-up and prognostic factor analysis in advanced ovarian carcinoma: the gynecologic oncology group experience. J Clin Oncol 1991;9:1138–50.

4. Kaufmann M, Von Minckwitz G, Kuhn W, et al. Combination of new biologic parameters as prognostic index in epithelial ovarian carcinoma. Int J Gynecol Cancer 1995;5:49–55.

5. Akahira J, Inoue T, Suzuki T, et al. Progesterone receptor isoforms A and B in human epithelial ovarian carcinoma: immunohistochemical and RT-PCR studies. Br J Cancer 2000;83:1488–94.

6. Cooper BC, Sood AK, Davis CS, et al. Pre-operative CA125 levels: an independent prognostic factor for epithelial ovarian cancer. Obstet Gynecol 2002;100:59–64.

7. Miki Y, Swensen J, Shattuck-Eidens D, et al. A strong candidate for the breast and ovarian cancer susceptibility gene BRCA1. Science (Wash DC) 1994;266:66–71.

8. Wooster R, Bignell G, Lancaster J, et al. Identification of the breast cancer susceptibility gene BRCA2. Nature (Lond) 1995;378:789–92.

9. Guttmacher AE, Collins FS. Breast and ovarian cancer. N Engl J Med 2003;348:2339–47.

10. Newman B, Millikan RC, King MC. Genetic epidemiology of breast and ovarian cancers. Epidemiol Rev 1997;19:69–79.

11. Ford D, Easton DF, Peto J. Estimates of the gene frequency of BRCA1 and its contribution to breast and ovarian cancer incidence. Am J Hum Genet 1995;57:1457–62.

12. Kass SU, Pruss D, Wolffe AP. How does DNA methylation repress transcription? Trends Genet 1997;13:444–9.

13. Razin A, Ceder H. DNA methylation and gene expression. Microbiol Rev 1991;55:451–8.

14. Jones PA, Laird PW. Cancer epigenetics comes of age. Nat Genet 1999;21:163–7.

15. Esteller M, Corn PG, Baylin SB, Herman JG. A gene hypermethylation profile of human cancer. Cancer Res 2001;61:3225–9.

16. Hermeking H, Lengauer C, Polyak K, et al. 14-3-3σ is a p53-regulated inhibitor of G_2/M progression. Mol Cell 1997;1:3–11.

17. Chan TA, Hermeking H, Langauer C, Kinzler KW, Vogelstein B. 14-3-3σ is required to prevent mitotic catastrophe after DNA damage. Nature (Lond) 1999;401:616–20.

18. Ferguson AT, Evron E, Umbricht CB, et al. High frequency of hypermethylation at the 14-3-3σ locus leads to gene silencing in breast cancer. Proc Natl Acad Sci USA 2000;97:6049–54.

19. Suzuki H, Itoh F, Toyota M, et al. Inactivation of the 14-3-3σ gene is associated with 5′ CpG island hypermethylation in human cancers. Cancer Res 2000;60:4353–7.

20. Osada H, Tatematsu Y, Yatabe Y, et al. Frequent and histological type-specific inactivation of 14-3-3σ in human lung cancers. Oncogene 2002;21:2418–24.

21. WHO. Handbook for reporting results of cancer treatment. WHO Publication No. 48. Geneva: WHO; 1979.

22. Shimizu Y, Kamoi S, Amada S, et al. Toward the development of a universal grading system for ovarian epithelial carcinoma. Prognostic significance of histopathologic features-problems involved in the architectural grading system. Gynecol Oncol 1998;70:2–12.

23. Nitta M, Katabuchi H, Ohtake H, et al. Characterization and tumorigenicity of human ovarian surface epithelial cells immortalized by SV40 large T antigen. Gynecol Oncol 2001;81:10–7.

24. Herman JG, Graff JR, Myohanen S, Nelkin BD, Baylin SB. Methylation-specific PCR: a novel PCR assay for methylation status of CpG islands. Proc Natl Acad Sci USA 1996;93:9821–6.

25. Akahira J, Suzuki T, Ito K, et al. Differential expression of progesterone receptor isoforms A and B in the normal ovary, and in benign, borderline, and malignant ovarian tumors. Jpn J Cancer Res 2002;93: 807–15.

26. Akahira J, Suzuki T, Ito K, et al. Expression of 5α-reductases in human epithelial ovarian cancer: its correlation with androgen receptor status. Jpn J Cancer Res 2001;92:926–32.

27. Lodygin D, Yazdi AS, Sander CA, Herzinger T, Hermeking H. Analysis of 14-3-3σ expression in hyperproliferative skin diseases reveals selective loss associated with CpG-methylation in basal cell carcinoma. Oncogene 2003;22:5519–24.

28. Dhar S, Squire JA, Hande MP, Wellinger RJ, Pandita TK. Inactivation of 14-3-3σ influences telomere behavior and ionizing radiation-induced chromosomal instability. Mol Cell Biol 2000;20:7764–72.

29. Lengauer C, Kinzler KW, Vogelstein B. Genetic instability in human cancers. Nature (Lond) 1999;396:643–9.

30. Ostergaard M, Rasmussen HH, Nielsen HV, et al. Proteome profiling of bladder squamous cell carcinomas: identification of markers that define their degree of differentiation. Cancer Res 1997;57:4111–7.

31. Umbricht CB, Evron E, Gabrielson E, et al. Hypermethylation of 14-3-3σ (stratifin) is an early event in breast cancer. Oncogene 2001; 20:3348–53.

32. Ahuja N, Li Q, Mohan AL, Baylin SB, Issa JP. Aging and DNA methylation in colorectal mucosa and cancer. Cancer Res 1998;58: 5489–94.

33. Issa JP. CpG-island methylation in aging and cancer. Curr Top Microbiol Immunol 2000;249:101–18.

34. Iggo R, Gatter K, Bartek J, Lane D, Harris AL. Increased expression of mutant forms of p53 oncogene in primary lung cancer. Lancet 1990;335:675–9.

35. Skilling JS, Sood A, Niemann T, Lager DJ, Buller RE. An abundance of p53 null mutations in ovarian carcinoma. Oncogene 1996;13: 117–23.

Available online at www.sciencedirect.com
SCIENCE DIRECT®
Biochemical and Biophysical Research Communications 325 (2004) 1312–1317
BBRC
www.elsevier.com/locate/ybbrc

Identification and functional analysis of consensus androgen response elements in human prostate cancer cells☆

Kuniko Horie-Inoue[a], Hidemasa Bono[b], Yasushi Okazaki[b], Satoshi Inoue[a,c,*]

[a] *Division of Gene Regulation and Signal Transduction, Research Center for Genomic Medicine, Saitama Medical School, 1397-1 Yamane, Hidaka-shi, Saitama 350-1241, Japan*

[b] *Division of Functional Genomics and Systems Medicine, Research Center for Genomic Medicine, Saitama Medical School, 1397-1 Yamane, Hidaka-shi, Saitama 350-1241, Japan*

[c] *Department of Geriatric Medicine, Faculty of Medicine, The University of Tokyo, 7-3-1 Hongo, Bunkyo-ku, Tokyo 113-8655, Japan*

Received 26 October 2004
Available online 11 November 2004

Abstract

Androgen receptor (AR) recognizes and binds to 15-bp palindromic androgen response element (ARE) sequences with high affinity in vitro, which consist of two hexameric half-sites arranged as inverted repeats with a 3-bp spacer. Although a few near-consensus ARE sequences have been actually identified in the transcriptional regulatory regions of androgen-responsive genes, it has been unclear whether the exact consensus sequences function as bona fide AREs in vivo. A genome-wide in silico screening of palindromic AREs identified 563 exact consensus sequences in the human genome. The distribution of perfect palindromic AREs among the chromosomes is basically consistent with the length of chromosomes. Using human prostate cancer cell line LNCaP treated with a synthetic androgen R1881 as a model, in vivo AR binding abilities of 21 consensus AREs were analyzed by chromatin immunoprecipitation. Of 21 genomic fragments containing perfect AREs in chromosome X, 8 fragments recruited more ARs (>4-fold enrichment) even compared with the proximal ARE region of prostate-specific antigen. A couple of proximal genes or putative transcripts in the vicinity of the perfect AREs were found to be androgen-responsive analyzed by quantitative RT-PCR. Our results suggest that some of perfect palindromic AREs could function as in vivo AR binding sites in the human genome and regulate gene transcription.
© 2004 Elsevier Inc. All rights reserved.

Keywords: Androgen receptor; Androgen response element; Androgen-responsive gene; Chromatin immunoprecipitation; Prostate cancer

The androgen receptor (AR), a member of nuclear receptor superfamily that functions as a ligand-dependent transcription factor, plays an essential role in male sexual differentiation as well as prostate development and carcinogenesis. Forming complexes with coactivators and general transcription factors, ligand-stimulated AR binds to *cis*-acting androgen response elements (AREs) in the regulatory regions of androgen-responsive genes and modulates the transcription of target genes. The palindromic 15-bp sequence, which consists of two hexameric half-sites (5′-AGAACA-3′) arranged as an inverted repeat with a 3-bp spacer, has been identified as the consensus sequence for AR binding [1,2]. Although near-consensus ARE sequences that match at least 9 of 12 nucleotides have been found in the regulatory regions of several androgen-responsive genes [1], none of the perfect consensus ARE has yet been identified. A question arises whether the palindromic ARE consensus sequence functions as a bona fide AR binding

☆ *Abbreviations:* AR, androgen receptor; ARE, androgen response element; BCOR, BCL-6 interacting corepressor; ChIP, chromatin immunoprecipitation; GAPDH, glyceraldehyde-3-phosphate dehydrogenase; PCYT1B, phosphorylcholine transferase B; PSA, prostate-specific antigen; RT-PCR, reverse transcription-polymerase chain reaction.

* Corresponding author. Fax: +81 3 5800 6530.
E-mail address: INOUE-GER@h.u-tokyo.ac.jp (S. Inoue).

0006-291X/$ - see front matter © 2004 Elsevier Inc. All rights reserved.
doi:10.1016/j.bbrc.2004.10.174

site that regulates transcription of proximal androgen-responsive genes in vivo.

In the present study, we identified perfect ARE sites in silico based on the human genome sequences that are available from public database and analyzed experimentally the functions of consensus AREs in terms of AR binding abilities in vivo and potential androgen-dependent transcription regulation of proximal genes. Focusing on the chromosome X, we actually identified several AR binding sites among the computationally identified perfect ARE sequences. A couple of proximal RNA transcripts in the vicinity of perfect AREs were androgen-responsive, suggesting that some of the consensus ARE sites have potentials to activate transcription of nearby genes. Our combined approach of characterization of ARE sites will contribute to the systematic elucidation of the gene regulatory network mediated by androgen, which will be pivotal for the development of prostate cancer.

Materials and methods

Bioinformatics. Consensus AREs in the human genome (Human 34d Gene Build retrieved from Ensembl ftp site [3]) were screened utilizing in-house Perl script and a program for regular expression search of a nucleotide sequence (program name: dreg) in EMBOSS package [4]. The regular expression pattern for ARE was obtained from a recent literature by Nelson et al. [1], in which the palindromic 5′-AGAACAnnnTGTTCT-3′ sequence corresponding to the ARE sequence in TRANSFAC database [5] was used as a consensus sequence.

Cell culture. Human prostate cancer LNCaP cells were purchased from American Type Culture Collection (Rockville, MD) and maintained in RPMI 1640 supplemented with 4.5 g/dl glucose, 1 mM sodium pyruvate, 10 mM Hepes, and 10% fetal bovine serum (FBS). Prior to hormone addition, cells were cultured for 2 days in phenol red-free RPMI 1640 supplemented with 5% dextran–charcoal stripped FBS (dcc-FBS) and one day in phenol red-free RPMI 1640 supplemented with 2.5% dcc-FBS.

Chromatin immunoprecipitation assay. LNCaP cells (8×10^7) after 72-h hormone depletion were treated with 10 nM of R1881 (NEN Life Science Products, Boston, MA) or 0.1% ethanol for 24 h. Cells were fixed in 1% formaldehyde for 5 min at room temperature. Chromatin was sheared to an average size of 500 bp by sonication using a Bioruptor ultrasonicator (Cosmo-Bio, Tokyo, Japan). Lysates corresponding to 2×10^7 cells were rotated at 4 °C for overnight with 3 μg of polyclonal anti-AR antibody (H-280, Santa Cruz Biotechnology, Santa Cruz, CA) or non-specific rabbit IgG (Sigma). Salmon sperm DNA/protein A–agarose (Upstate Biotechnology, Lake Placid, NY) was added and incubated for 2 h. Washing and reversal of cross-links was performed as described [6]. Precipitated DNA fragments were quantified by quantitative real-time PCR using the Applied Biosystems 7000 sequence detector (Foster City, CA) based on SYBR Green I

Table 1
Primers for quantitative ChIP assay and RT-PCR

Target	Forward primer sequence	Reverse primer sequence
ARE sites[a]		
X1	5′-GTGCTTTGCAGGCAGTGATG-3′	5′-TCATTCCTTTGTTTTACTGAGAGTTCA-3′
X2	5′-GCAACTGCAAAGCCAAAATG-3′	5′-ATCTGTTTCCCATCTCCGTATATGTA-3′
X3	5′-CCAAAAAGCCCCTAGGAAAGA-3′	5′-AACCAGCAGTGTTTGCTCCAA-3′
X4	5′-CCAGGGCTCCTCCTTTGG-3′	5′-ATCTGACCCTGTGCATTTGAGA-3′
X5	5′-ACAGGTGCAAACACACAAAAGC-3′	5′-ACCCTTTCCTGGTCCTTTGTC-3′
X6	5′-ACAACAAATTCACCTGAGGTTCATAT-3′	5′-GCTTATCCAGGGACATCAGGTT-3′
X7	5′-CCAAATATGTCCATTCATCCAACA-3′	5′-GGAAACATACGCATTGCCTAGAA-3′
X8	5′-TTAATGTCTCTGTGAACCATTCTTCTG-3′	5′-GGTAACTACTGGGAAGGGAATTAGC-3′
X9	5′-CTGAGGGCGGACCTTGTTAAG-3′	5′-GCTCCAGGAGCTCTACGAGGTT-3′
X10	5′-TTAACAAAAAGCCAAGAGTGACAA-3′	5′-ACATCTTTTTTTCTTTGCTCCAGAA-3′
X11	5′-GAAGGTCCGTTGAGTTTATCTATTC-3′	5′-GGAAGTTTTCAGACATTTCTTCAG-3′
X12	5′-TGTGTAAAACACTCAACAAGTTAGAACA-3′	5′-CCTTGCCTTCTTTCTGATCTTAGG-3′
X13	5′-CGGGCAGTGGAAAAGCAA-3′	5′-CCTGTGTCTCCTCAAAAGAAATGA-3′
X14	5′-CAGTTCTGATGTGGTAAGTGGAAGA-3′	5′-GGTGAGTGGCGAAGTGGTAAC-3′
X15	5′-TCCCAGTTTCTCAGGGATCACT-3′	5′-TCTCCCACATGAAACAACTAAAAAGT-3′
X16	5′-AGGGCCAGCTTTATTAAGAACAGA-3′	5′-CTGTAGGAGCCCTGCAAGGT-3′
X17	5′-AATGTTTGCTTACTGCAAGTGTACT-3′	5′-GTGTGGGTTGCATGTACTGC-3′
X18	5′-TTTTGTCCCAGTCCTACATCTTGTT-3′	5′-GCTCATGTCCTCTATAGCCCTACA-3′
X19	5′-GCAGATTTTAAACCACAGTATTAAGTCAAA-3′	5′-GAGGGTACAGAGGAGCCAAAGA-3′
X20	5′-CAGAATCTGTAGCCAAACTACGAACT-3′	5′-CAGCCTGGCCCTTTTACTGA-3′
X21	5′-TCCTAGGAGAAATGGCTGATTCC-3′	5′-CAAAGTGTCATTATTCAGTGTACAACTCTAC-3′
PSA proximal promoter	5′-TCTGCCTTTGTCCCCTAGAT-3′	5′-AACCTTCATTCCCCAGGACT-3′
PSA distal promoter	5′-ACAGACCTACTCTGGAGGAAC-3′	5′-AAGACAGCAACACCTTTTT-3′
PSA coding	5′-GCCCTGCCCGAAAGG-3′	5′-GATCCACTTCCGGTAATGCA-3′
GAPDH coding[b]	5′-GGTGGTCTCCTCTGACTTCAACA-3′	5′-GTGGTCGTTGAGGGCAATG-3′
PCYT1B coding	5′-GCAGGGATGTTCGTTCCAA-3′	5′-CTGGTAATGATGTCCGATGTTGA-3′
NM_144657 coding	5′-CAGCAACAACAGGAACCTCTTTG-3′	5′-CGAGCAATATTAACCACATTTCTGA-3′
Genscan00000043157[c]	5′-GACAGTAGACTTCCCAGAGCACATAG-3′	5′-TCTCCTGTTTCAGTCCAATTCTGA-3′

[a] The position of ARE sites are described in Table 2.
[b] Primers for GAPDH coding were used for both ChIP assay and RT-PCR.
[c] Genscan00000043157: a putative transcript predicted by the Ensembl pipeline analysis system using the Genscan prediction program.

fluorescence. Primer pairs were designed by Primer Express ver. 2.0 software (Applied Biosystems), generating perfect ARE-containing fragments with the requirements of primer T_m temperature at basically 58–60 °C and the requirements of amplicon length for 50–150 bp. The protocol of PCR was 2 min at 50 °C, 10 min at 95 °C, and 40 cycles of 15 s at 95 °C and 1 min at 60 °C. To determine relative differences among the treatment groups for the chromatin immunoprecipitation (ChIP) assays we used the $\Delta\Delta C_t$ method as outlined in the Applied Biosystems protocol for reverse transcriptase-PCR. The average threshold cycle (C_t) for the duplicate was used in all subsequent calculations. A genomic fragment corresponding to GAPDH was used as an external standard. Genomic fragments containing proximal or distal ARE in the promoter region of prostate-specific antigen (PSA) (−250 to −39 bp and −4170 to −3978 bp from the transcriptional initiation site, respectively) [6] were used as positive controls. The sequences of the primers used in ChIP assays (synthesized by Sigma Genosys, Japan) are described in Table 1.

Quantitative reverse transcription-PCR. Total RNA was extracted from R1881-treated or 0.1% ethanol-treated LNCaP cells for 24 h using ISOGEN reagent (Nippon Gene, Tokyo, Japan). First strand cDNA was generated from RNase-free DNase I-treated total RNA by using SuperScript II Reverse Transcriptase (Invitrogen, Carlsbad, CA) and $pdT_{12\ 18}$ primer (Amersham Biosciences, Piscataway, NJ). Proximal genes or putative transcripts that locate within a ±20-kb distance from perfect AREs were selected for reverse transcription-PCR (RT-PCR) analysis. cDNAs were quantified by quantitative real-time PCR using the Applied Biosystems 7000 sequence detector based on SYBR Green I fluorescence as described above. The primer sequences for the amplifications are described in Table 1.

Results

In silico identification of perfect palindromic ARE sequences in the human genome

In terms of palindromic ARE sequences composed of two AGAACA sequences separated by a 3-bp spacer, a few near-consensus sequences, but no perfect palindromic sequences have been identified among human androgen-responsive genes. In order to answer the question whether perfect palindromic ARE sequences do function as in vivo AR binding sites, we computationally searched all the consensus ARE sequences in the human genome utilizing in-house Perl script and a program for regular expression pattern search of a nucleotide sequence in EMBOSS package (program name: dreg) [4]. The screening defined 563 elements, noting that the number of sites was larger than the expected frequency in random DNA sequences as calculated by the total number of base pairs in the genome divided by the frequency of a sequence with specified base pairs at 12 positions ($3{,}223{,}443{,}491/4^{12} = 192$). The distribution of consensus sequences among the chromosomes is generally consistent with chromosomal size, the average frequency of ARE being 17.3 ± 4.3 sites per 100 Mb (Figs. 1A and B).

In vivo AR recruitment of perfect AREs on chromosome X

To investigate whether the computationally identified ARE sequences with perfect motifs recruit AR in vivo, we performed ChIP assay in AR-positive LNCaP cells. The chromosome X was selected as an experimental model, in which AR gene itself locates. The distribution of 21 perfect ARE sites on chromosome X is mapped in Fig. 2 and the detailed information of ARE (X1–X21) sites including nucleotide positions and sequences is in Table 2. None of the consensus AREs clustered in chromosome X within 50 kb, as the narrowest distance between X5 and X6 was 57.7 kb.

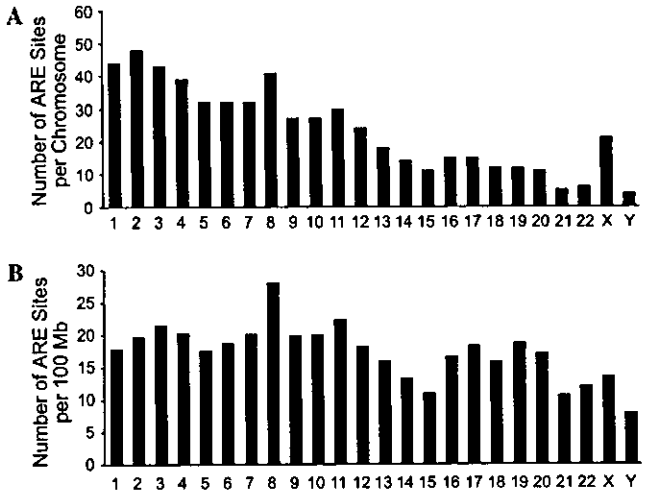

Fig. 1. Distribution of perfect palindromic AREs in the human genome. (A) The number of perfect consensus AREs found per chromosome. (B) The ratio between the number of perfect AREs and the length of chromosome (sites per 100 Mb).

We performed quantitative PCR using genomic DNAs from LNCaP cells with 24-h treatment of R1881 (10 nM) or 0.1% ethanol, immunoprecipitated by either a specific AR antibody or non-specific rabbit IgG (Fig. 3). The AR association with proximal and distal promoter regions of PSA including ARE sequences was more than 3.5-fold and 60-fold increased by R1881 treatment, respectively. Of 21 genomic fragments containing perfect AREs in chromosome X, 8 fragments recruited more ARs (>4-fold enrichment) compared with the proximal ARE region of PSA. No particular specificity of 3-bp spacer sequences for AR recruitment has been found; for example, both ARE X5 and X6 sites contain a GCC spacer while fold enrichment of AR recruitment was 1.2-fold and 7.2-fold, respectively. In the case of X17 and X19 sites possessing an identical GCA spacer, fold difference of AR binding was 9.5-fold and 2.0-fold, respectively.

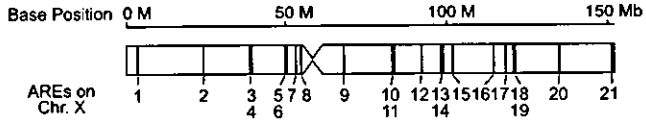

Fig. 2. Positions of the perfect palindromic AREs on chromosome X. Indicated numbers 1–21 correspond to perfect ARE sites.

Table 2
Proximal RNA transcripts in the vicinity of perfect palindromic AREs in chromosome X

AREID[a]	Start	Stop	ARE sequence	Proximal transcript	Ensembl ID No.	Location of ARE site[b]
X1	3181583	3181597	AGAACAtggTGTTCT	PRKX	ENSG00000183943	Within
X2	23945954	23945968	AGAACActaTGTTCT	PCYT1B	ENSG00000102230	Within
X3	38720672	38720686	AGAACAaagTGTTCT	*Ab-initio* Genscan transcript[c]	GENSCAN00000046001	Within
X4	38970910	38970924	AGAACAaagTGTTCT	BCOR	ENSG00000183337	5′ (3 kb)/within[d]
X5	49168004	49168018	AGAACAgccTGTTCT	*Ab-initio* Genscan transcript	GENSCAN00000107032	3′ (8 kb)
X6	49225713	49225727	AGAACAgccTGTTCT	*Ab-initio* Genscan transcript	GENSCAN00000043157	3′ (10 kb)
X7	52321185	52321199	AGAACAttaTGTTCT	O60275	ENSG00000124313	5′ (4 kp)
X8	53952953	53952967	AGAACAtaaTGTTCT	PFKFB1	ENSG00000158571	Within
X9	67507044	67507058	AGAACAgaaTGTTCT	*Ab-initio* Genscan transcript	GENSCAN00000115882	Within
X10	82472510	82472524	AGAACAatgTGTTCT	NM_144657	ENSG00000165259	Within
X11	83327890	83327904	AGAACAttcTGTTCT	NM_024921	ENSG00000124429	Within
X12	91506977	91506991	AGAACAaaaTGTTCT	*Ab-initio* Genscan transcript	GENSCAN00000029252	Within
X13	98772894	98772908	AGAACAagaTGTTCT	SYTL4	ENSG00000102362	5′ (5 kb)
X14	98951387	98951401	AGAACAtctTGTTCT	Ensembl novel transcript	ENST00000328526	Within
X15	101412450	101412464	AGAACAgctTGTTCT	NGFRAP1	ENSG00000166681	3′ (8 kb)
X16	114061336	114061350	AGAACAgaaTGTTCT	*Ab-initio* Genscan transcript	GENSCAN00000064921	Within
X17	118442517	118442531	AGAACAgcaTGTTCT	CUL4B	ENSG00000158290	Within
X18	120798222	120798236	AGAACActaTGTTCT	*Ab-initio* Genscan transcript	GENSCAN00000054945	Within
X19	121144935	121144949	AGAACAgcaTGTTCT	GRIA3	ENSG00000125675	Within
X20	134752049	134752063	AGAACAactTGTTCT	Q96NB7	ENSG00000173971	Within
X21	151348988	151349002	AGAACAcccTGTTCT	NM_152274	ENSG00000147382	5′ (16 kb)

[a] ARE ID X1–X21 correspond to the numbers 1–21 in Fig. 2.
[b] Location of ARE site indicates the proximity to annotated genes or putative transcripts.
[c] *Ab-initio* Genscan transcript: putative transcript predicted by the Ensembl pipeline analysis system using the Genscan prediction program [7].
[d] BCOR has two different initiation sites.

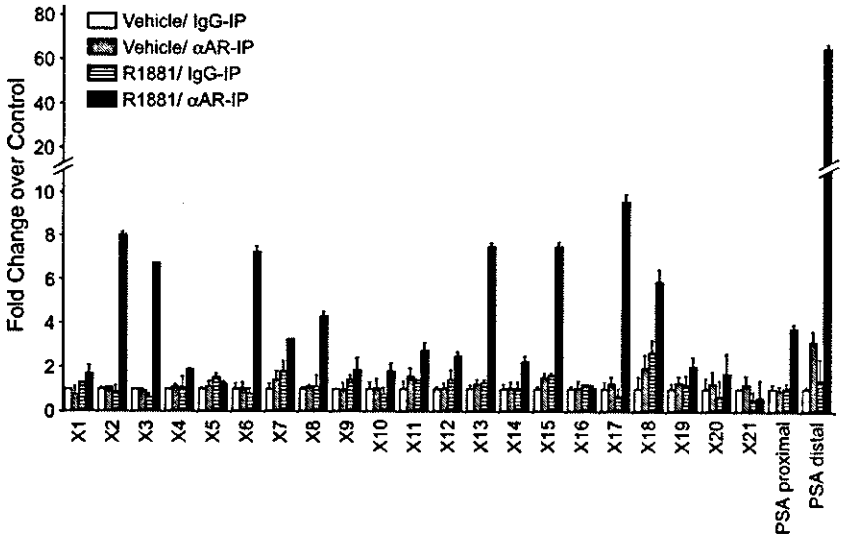

Fig. 3. Chromatin immunoprecipitation assay in LNCaP cells. Cells after 72-h hormone depletion were treated with 10 nM R1881 or 0.1% ethanol as a vehicle for 24 h. Quantitative PCR was performed using ChIP DNA samples immunoprecipitated by rabbit polyclonal anti-AR antibody (αAR-IP) or non-specific rabbit IgG (IgG-IP). In each case, fold enrichment values in R1881-treated samples immunoprecipitated by anti-AR antibody and non-specific rabbit IgG (R1881/αAR-IP and R1881/IgG-IP) as well as vehicle-treated ones precipitated by anti-AR antibody (vehicle/αAR-IP) were compared with those in vehicle-treated samples precipitated by non-specific rabbit IgG (vehicle/IgG-IP). Each result is the mean ± SEM of two independent experiments in duplication (four determinants). Prostate-specific antigen (PSA) proximal and distal promoter regions are served as positive controls.

Potential transcriptional regulation of proximal genes in the vicinity of perfect AREs

To examine whether perfect AREs regulate transcriptional activities of proximal genes, we next performed quantitative RT-PCR for RNA transcripts in the vicinity of consensus ARE sites. Proximal genes were selected for each ARE site based on the following requirements of ARE location: (1) within an annotated gene, (2) within 20-kb upstream to 5′ end of a known gene, or (3)

within 20-kb downstream to 3′ terminus of a known gene (Table 2). If no annotated genes exist in the vicinity of ARE sites, putative transcripts predicted by the Ensembl pipeline analysis system using the Genscan prediction program [7] and mapped on the Ensembl genome browser were chosen (i.e., *ab-initio* Genscan transcripts). Ten out of 21 AREs are located within introns of known genes or a novel transcript, 4 sites in the 5′ regions of annotated genes [ARE X4 is counted in both 5′ region and within intron 1 of BCOR (BCL-6 interacting corepressor) due to variants], one site in the 3′ regions of a known gene. No known genes were found in the vicinity of seven ARE sites.

Quantitative RT-PCR was conducted using the first-strand cDNAs derived from LNCaP cells treated with a synthetic androgen R1881 or 0.1% ethanol as a vehicle for 24 h. Two annotated genes and one putative transcript exhibited significant increase in transcript expression levels agonist-dependently (Fig. 4). PCYT1B (phosphorylcholine transferase B) is a gene encoding an enzyme that controls phosphatidylcholine synthesis [8,9]. PCYT1B may be related to the reproduction function as it is highly expressed in testis, placenta, and ovary. Perfect ARE (X2) locates within intron 7 of PCYT1B. In regard to NM_144657, the gene encodes 690 amino acids and contains perfect ARE (X10) within intron 3. Although the fold enrichment of R1881-activated AR binding in ARE X10 was smaller than that in the PSA proximal promoter region, yet it is statistically significant ($P < 0.05$). The gene NM_144657 is found to possess two HOX homeobox domains by analyzing domain architectures using a Simple Modular Architecture Research Tool (SMART) on InterPro databases (http://www.ebi.ac.uk/interpro/databases.html). The gene may be a nuclear DNA-binding protein that is involved in the transcriptional regulation of developmental processes. Concerning an *ab-initio* Genscan transcript (ID: Genscan00000043157) that is located 10-kb upstream to consensus ARE (X6), the sequence does not exhibit overall similarity with any characterized human gene.

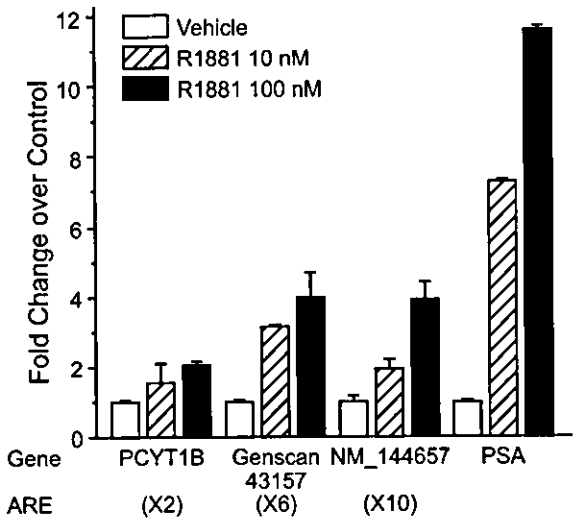

Fig. 4. Quantitative RT-PCR of proximal genes in the vicinity of perfect AREs. LNCaP cells after 72-h hormone depletion were treated with R1881 (10 or 100 nM) or 0.1% ethanol as a vehicle for 24 h. Real-time PCR was conducted using the first strand cDNAs generated from the total RNAs of the cells. PCYT1B, Genscan43157 (Genscan00000043157), and NM_144657 are located in the vicinity of ARE X2, X6, and X10, respectively. Each result is the mean ± SEM of two independent experiments in duplication (four determinants). PSA is served as a positive control.

Discussion

In the present study, we identified 563 perfect palindromic ARE sequences in the human genome, whose frequency of occurrence is more than our initial expectation of approximately 200 sites. We functionally analyzed 21 consensus AREs on chromosome X as a sample of the population. Eight of 21 AREs recruited more ARs (>4-fold enrichment) upon ligand treatment even compared with the proximal ARE region of PSA, as determined by ChIP assay using human prostate cancer LNCaP cells. It was also shown that distal ARE region of PSA showed by far the highest recruitment of AR. In regard to the expression of transcripts that locate with ±20 kb from perfect AREs, two annotated genes and one putative transcript were upregulated ligand-dependently, suggesting that these proximal genes are potentially androgen-responsive genes.

Our results reveal two interesting points in the field of steroid receptors. One is the frequency of occurrence of hormone response elements. Based on our data of ChIP assay along chromosome X, there might be at least 200 perfect ARE sequences that actually function as AR binding sites in the entire human genome. A recent computational analysis of near-consensus estrogen response elements, in which 10 specified nucleotides and 2 nucleotide choices at 2 positions out of 12 bp, revealed that there are approximately 70,000 sequences in the human and mouse genomes [10]. By the experimental approach of tiling array of chromosomes 21 and 22 hybridized with immunoprecipitated DNAs, there might be large number of transcription factor binding sites with a minimal estimate of 12,000 for Sp1, 25,000 for c-Myc, and 1600 for p53 [11]. Taking together our present results and the estimation of transcription factors by others, there may be at least several thousand sites of functional AREs in the human genome.

The second interesting point is the relationship of perfect AREs to proximal genes and potential transcription regulation by consensus AREs. In our results, nearly half of the perfect AREs (10 of 21) on chromosome X are located within introns of annotated genes

including one novel transcript. The frequency of AREs within known genes is much higher than that of AREs in 5′ regions of annotated genes (4 of 21). In the case of transcription factor binding sites on chromosomes 21 and 22, 36% of these regions are situated within known genes or proximal to the 3′ most exon of a gene and the frequency was also higher than that of binding sites within 5′ to known genes (22%) [11]. As for NF-κB binding sites on chromosome 22, 40% of the regions are located in intronic sequences [12]. Indeed, there is evidence that several intronic DNA elements for NF-κB are functionally important in the gene regulation by co-operating with other DNA elements [13,14]. Thus, some of the consensus ARE sequences within annotated genes may be functional in the transcriptional regulation of those genes. Yet, those intronic binding sites are interesting in terms of the potential for distal regulatory elements or promoters for non-coding transcripts or antisense transcripts overlapping the 3′ untranslated regions.

In regard to consensus ARE sequences in unannotated regions, 7 of 21 sites are in regions more than ±20 kb apart from any annotation or novel transcribed regions. Six of 7 sites in unannotated regions are located within regions corresponding to *ab-initio* Genscan transcripts. The remaining one site (X6) is situated at 10-kb downstream to the 3′ end of an *ab-initio* Genscan transcript, yet this ARE may be functional as it has a significant in vivo AR binding ability and the expression levels of the proximal *ab-initio* Genscan transcript (Genscan00000043157) are androgen-inducible. It is interesting to compare our results with NF-κB binding sites on chromosome 22 [12], as 22% of the binding sites for p65 lie in regions more than 50 kb from any annotation. Taken together, our results suggest that there are many unannotated regions that include transcription factor binding sites and have biological functions.

Concerning the differences in binding potency among AREs, several factors such as the nearby chromosomal environment or the chromatin accessibility of specific co-operating factors as well as basal transcriptional factors may be involved. Future comparative studies with different cell context will reveal the variations of chromatin structure and contribute to the identification of novel androgen-responsive genes that are critically involved in the development of prostate cancer.

In summary, the present study demonstrates the usefulness of the genome-wide approach combined with computational analysis and experimental verification in hormone-responsive genes. Our functional analysis reveals that some of the perfect AREs are actual AR binding sites in vivo and may relate to the transcription regulation of proximal genes. Our study will mark the first step toward the elucidation of the entire gene regulatory network mediated by androgen.

Acknowledgments

We thank Y. Suzuki and R. Nozawa for their technical assistance. This work was supported by Grants-in-Aid for Scientific Research under Category "S" and Scientific Research in Priority Areas "Cancer Research" and "Genome Science" from the Ministry of Education, Culture, Sports, Science and Technology of Japan.

References

[1] P.S. Nelson, N. Clegg, H. Arnold, C. Ferguson, M. Bonham, J. White, L. Hood, B. Lin, The program of androgen-responsive genes in neoplastic prostate epithelium, Proc. Natl. Acad. Sci. USA 99 (2002) 11890–11895.

[2] P.L. Shaffer, A. Jivan, D.E. Dollins, F. Claessens, D.T. Gewirth, Structural basis of androgen receptor binding to selective androgen response elements, Proc. Natl. Acad. Sci. USA 101 (2004) 4758–4763.

[3] E. Birney, D. Andrews, P. Bevan, M. Caccamo, G. Cameron, Y. Chen, L. Clarke, G. Coates, T. Cox, J. Cuff, et al., Ensembl 2004, Nucleic Acids Res. 32 (2004) D468–D470.

[4] P. Rice, I. Longden, A. Bleasby, EMBOSS: the european molecular biology open software suite, Trends Genet. 16 (2000) 276–277.

[5] V. Matys, E. Fricke, R. Geffers, E. Gossling, M. Haubrock, R. Hehl, K. Hornischer, D. Karas, A.E. Kel, O.V. Kel-Margoulis, et al., TRANSFAC: transcriptional regulation, from patterns to profiles, Nucleic Acids Res. 31 (2003) 374–378.

[6] Y. Shang, M. Myers, M. Brown, Formation of the androgen receptor transcription complex, Mol. Cell 9 (2002) 601–610.

[7] C. Burge, S. Karlin, Prediction of complete gene structures in human genomic DNA, J. Mol. Biol. 268 (1997) 78–94.

[8] A. Lykidis, I. Baburina, S. Jackowski, Distribution of CTP:phosphocholine cytidylyltransferase (CCT) isoforms. Identification of a new CCT splice variant, J. Biol. Chem. 274 (1999) 26992–27001.

[9] A. Lykidis, K.G. Murti, S. Jackowski, Cloning and characterization of a second human CTP:phosphocholine cytidylyltransferase, J. Biol. Chem. 273 (1998) 14022–14029.

[10] V. Bourdeau, J. Deschenes, R. Metivier, Y. Nagai, D. Nguyen, N. Bretschneider, F. Gannon, J.H. White, S. Mader, Genome-wide identification of high-affinity estrogen response elements in human and mouse, Mol. Endocrinol. 18 (2004) 1411–1427.

[11] S. Cawley, S. Bekiranov, H.H. Ng, P. Kapranov, E.A. Sekinger, D. Kampa, A. Piccolboni, V. Sementchenko, J. Cheng, A.J. Williams, R. Wheeler, B. Wong, J. Drenkow, M. Yamanaka, S. Patel, S. Brubaker, H. Tammana, G. Helt, K. Struhl, T.R. Gingeras, Unbiased mapping of transcription factor binding sites along human chromosomes 21 and 22 points to widespread regulation of noncoding RNAs, Cell 116 (2004) 499–509.

[12] R. Martone, G. Euskirchen, P. Bertone, S. Hartman, T.E. Royce, N.M. Luscombe, J.L. Rinn, F.K. Nelson, P. Miller, M. Gerstein, S. Weissman, M. Snyder, Distribution of NF-κB-binding sites across human chromosome 22, Proc. Natl. Acad. Sci. USA 100 (2003) 12247–12252.

[13] H. Schjerven, P. Brandtzaeg, F.E. Johansen, A novel NF-κB/Rel site in intron 1 cooperates with proximal promoter elements to mediate TNF-α-induced transcription of the human polymeric Ig receptor, J. Immunol. 167 (2001) 6412–6420.

[14] K. Maehara, T. Hasegawa, K.I. Isobe, A NF-κB p65 subunit is indispensable for activating manganese superoxide: dismutase gene transcription mediated by tumor necrosis factor-α, J. Cell. Biochem. 77 (2000) 474–486.

JOURNAL OF CELLULAR PHYSIOLOGY 203:193–201 (2005)

Survival Versus Apoptotic 17β-Estradiol Effect: Role of ERα and ERβ Activated Non-genomic Signaling

FILIPPO ACCONCIA,[1] PIERANGELA TOTTA,[1] SUMITO OGAWA,[2] IRENE CARDILLO,[1] SATOSHI INOUE,[2] STEFANO LEONE,[1] ANNA TRENTALANCE,[1] MASAMI MURAMATSU,[2] AND MARIA MARINO[1]*

[1]*Department of Biology, University "Roma Tre," Rome, Italy*
[2]*Research Center for Genomic Medicine, Saitama Medical School, Saitama, Japan*

The capability of 17β-estradiol (E2) to induce the non-genomic activities of its receptors (ERα and ERβ) and to evoke different signaling pathways committed to the regulation of cell proliferation has been analyzed in different cell cancer lines containing transfected (HeLa) or endogenous (HepG2, DLD1) ERα or ERβ. In these cell lines, E2 induced different effects on cell growth/apoptosis in dependence of ER isoforms present. The E2–ERα complex rapidly activated multiple signal transduction pathways (i.e., ERK/MAPK, PI3K/AKT) committed to both cell cycle progression and apoptotic cascade prevention. On the other hand, the E2–ERβ complex induced the rapid and persistent phosphorylation of p38/MAPK which, in turn, was involved in caspase-3 activation and cleavage of poly(ADP-ribose)polymerase, driving cells into the apoptotic cycle. In addition, the E2–ERβ complex did not activate any of the E2–ERα-activated signal molecules involved in cell growth. Taken together, these results demonstrate the ability of ERβ isoform to activate specific signal transduction pathways starting from plasma membrane that may justify the effect of E2 in inducing cell proliferation or apoptosis in cancer cells. In particular this hormone promotes cell survival through ERα non-genomic signaling and cell death through ERβ non-genomic signaling. J. Cell. Physiol. 203: 193–201, 2005.
© 2004 Wiley-Liss, Inc.

Knowledge of the molecular mechanism by which estrogens exert pleiotropic functions in different tissues and organs has evolved rapidly during the past two decades. In particular, the mechanism by which 17β-estradiol (E2) induces cell proliferation has been the object of extensive studies in several tissues (Sutherland et al., 1983; Marino et al., 1998, 2001; Castoria et al., 1999, 2001; Razandi et al., 1999). However, recent reports demonstrated that E2 could even decrease cell growth by significantly increasing apoptosis in breast cancer MCF-7 cell variants, prostate cells, and several other cell types (see Song and Santen, 2003 for review). Whether the E2 apoptotic effects can be explained by the expression of different estrogen receptor (ER) isoforms (i.e., ERα and ERβ) is presently unknown.

It has been assumed that E2 exerts survival proliferative effects mainly by rapid non-genomic mechanisms originating from the hormone binding to ERα (Marino et al., 1998, 2002; Castoria et al., 1999, 2001; Lobenhofer et al., 2000; Fernando and Wimalasena, 2004). In line with this assumption, E2 treatment of MCF-7 cells triggers association of ERα with Src kinase and p85, the regulatory subunit of PI3K, leading to DNA synthesis (Castoria et al., 2001). Moreover, E2 induces rapid non-genomic pathways and DNA synthesis even in ERα transiently transfected cell lines (e.g., Chinese hamster ovary, CHO; cervix epitheloid carcinoma cell line, HeLa) (Razandi et al., 1999; Marino et al., 2002). In addition, multiple and parallel signal transduction pathways are rapidly activated by the E2–ERα complex in hepatoma, HepG2, cells (e.g., ERK/MAPK, PI3K/AKT) (Marino et al., 2003). The disruption of such membrane starting pathways completely prevents the E2-induced DNA synthesis and the cyclin D_1 expression at the specific response elements, activator protein-1 (AP-1) and stimulating protein-1 (SP-1) (Marino et al., 2002, 2003). All these results point to the concept that ERα is the primary endogenous mediator of rapid E2 actions committed to cell proliferation.

Less information is available on the role played by ERβ in E2 proliferative effects. Data from cell cultures, gene expression, and knockout mice clearly indicate that E2-activated ERβ may function as a tumor suppressor by modulating the proliferative effects of ERα (Couse and Korach, 1999; Weihua et al., 2003; Cheng et al., 2004; Paruthiyil et al., 2004, Strom et al., 2004). These studies support a functional antagonism between ERα and ERβ with respect to the E2-induced cell proliferation, but do not clarify either the putative role of ERβ in E2-induced apoptosis or the signal transduction pathways involved. However, the ability of E2–ERβ complex to activate rapid non-genomic mechanisms has been reported. A subpopulation of ERβ transfected into CHO cells is membrane bound and capable of activating IP_3 production, ERK/MAPK and c-Jun kinase phosphorylation (Razandi et al., 1999). Recently, Geraldes and coworkers (Geraldes et al., 2003) reported that E2 reduces ERK/MAPK activity through ERβ stimulation in porcine smooth muscle cells. Moreover, conflicting

Abbreviations: E2, 17β-estradiol; E2-BSA, β-estradiol 6-(o-carboxy-methyl)oxime:BSA; ER, estrogen receptor; ERE, estrogen responsive element; ERK, extracellular regulated kinase; MAPK, mitogen-activated protein kinase; PI3K, phosphoinositide-3-kinase; PKC, protein kinase C; PARP, poly(ADP-ribose) polymerase.

Contract grant sponsor: MURST; Contract grant sponsor: University "Roma Tre"; Contract grant number: RBAU01TXN3_001; Contract grant sponsor: FIRB 2001 and 2004 University "Roma Tre".

*Correspondence to: Maria Marino, Department of Biology, University "Roma Tre," Viale G. Marconi, 446, I-00146 Rome, Italy. E-mail: m.marino@uniroma3.it

Received 4 June 2004; Accepted 29 July 2004

DOI: 10.1002/jcp.20219

© 2004 WILEY-LISS, INC.

evidences on the ability of ERβ to activate or inactivate Src and p38 kinases (Castoria et al., 2001; Kousteni et al., 2001; Geraldes et al., 2003; Mori-Abe et al., 2003) has been also reported. In particular, the existence of non-genomic mechanism(s) underling the antiproliferative effects of E2–ERβ complex is to date completely unknown.

Here, the ability of E2 to induce ERs activities has been studied in the HeLa cells devoid of any ERs and rendered E2-sensitive by transient transfection with human ERα or ERβ expression vectors. We report that E2 induced different effects on cell growth/apoptosis decision in the presence of the two different isoforms of receptor. The E2–ERα complex activated multiple signal transduction pathways (i.e., ERK/MAPK, PI3K/AKT, p38/MAPK) involved in cell cycle progression, whereas the E2–ERβ complex activated only p38/MAPK, which in turn, drives cells to apoptosis. A role of E2-induced ERK/MAPK activation in regulating some steps of the pro-apoptotic pathways is also demonstrated. These results were confirmed also in cancer cell lines expressing endogenous level of ERα or ERβ. Altogether our findings indicate a new action mechanism for the E2–ERβ complex pointing to the role of E2-induced rapid non-genomic signals in driving cell proliferation or apoptosis in cancer cells.

MATERIALS AND METHODS

Reagents

17β-estradiol, 17α-estradiol, L-glutamine, gentamicin, penicillin, RPMI-1640 and DMEM (without phenol red), charcoal-stripped fetal calf serum, and estradiol-BSA conjugate (β-estradiol 6-(o-carboxy-methyl)oxime:BSA, E2-BSA) were purchased from Sigma Chemical Co. (St. Louis, MO). The estrogen receptor inhibitor ICI 182,780 was obtained from Tocris (Ballwin, MO). The ERK/MAPK cascade inhibitor, U 0126, the PI3K inhibitor, Ly 294002, and the p38/MAPK inhibitor, SB 203580, were obtained from Calbiochem (San Diego, CA). Lipofectamine reagent was obtained from GIBCO-BRL Life-technology (Gaithersburg, MD). The luciferase kit was obtained from Promega (Madison, WI). GenElute plasmid maxiprep kit was obtained from Sigma Chemical Co. Bradford Protein Assay was obtained from BIO-RAD Laboratories (Hercules, CA). The policlonal anti-phospho-AKT, anti-phospho-p38, and anti-p38 antibodies were obtained by New England Biolabs (Beverly, MA); the policlonal anti-ERα, anti-ERβ, and anti-ERK and the monoclonal anti-phospho-ERK, anti-AKT, anti-Bcl-2, anti-caspase-3, anti-poly(ADP-ribose) polymerase (PARP), and anti-actin antibodies were obtained from Santa Cruz Biotechnology (Santa Cruz, CA). CDP-Star, chemiluminescence reagent for Western blot was obtained from NEN (Boston, MA).

All the other products were from Sigma Chemical Co. Analytical or reagent grade products, without further purification, were used.

Cell culture

The ER devoid human cervix epitheloid carcinoma cell line (HeLa) (Marino et al., 2002), the ERα containing hepatoma cell line (HepG2) (Marino et al., 2002, 2003; Moon et al., 2004), and the ERβ containing human colon adenocarcinoma cells (DLD1) (Fiorelli et al., 1999; Di Leo et al., 2001) were used as experimental models. Cells were routinely grown in air containing 5% CO_2 in modified, phenol red-free, DMEM (HeLa cells) or RPMI-1640 (HepG2 and DLD1 cells) media, containing 10% (v/v) charcoal-stripped fetal calf serum, L-glutamine (2 mM), gentamicin (0.1 mg/ml), and penicillin (100 U/ml). Cells were passaged every 2 days (HeLa and DLD1 cells) or every 4 days (HepG2 cells) and media changed every 2 days.

Plasmids and transfection procedures

The expression vectors for pCR3.1-β-galactosidase, human ERα (pSG5-HE0) (Marino et al., 2003), and human ERβ (pCNX2-ERβ) (Ogawa et al., 1998) have been used. Furthermore an empty vector, pCMV5, was used as control (Marino et al., 2001). Plasmids were purified for transfection using a plasmid preparation kit according to manufacturer's instructions. A luciferase dose response curve showed that the maximum effect was present when 1 μg of DNA was transfected in HeLa cells together with 1 μg of pCR3.1-β-galactosidase to normalize transfection efficiency (~55–65%). HeLa cells were grown to ~70% confluence, then transfected using Lipofectamine Reagent according to the manufacturer's instructions. Six hours after transfection the medium was changed and 24 h thereafter cells were stimulated with 10 nM E2.

Cell viability and cell cycle

HeLa cells were grown to ~70% confluence in 6-well plates, then transfected and, after 24 h, stimulated. At different times after treatment cells were harvested with trypsin and centrifuged. Cells were stained with trypan blue solution and counted in a hemocytometer (improved Neubauer chamber) in quadruplicate. For the cell cycle analysis, 10^6 cells were fixed with 1 ml ice-cold 70% ethanol and subsequently stained with 2 μg/ml DAPI/PBS solution. The fluorescence of DNA was measured with a DAKO Galaxy flow cytometer equipped with HBO mercury lamp and the percentage of cells present in sub-G1, G1, S, and G2/M phases was calculated using a FloMax© Software.

Electrophoresis and immunoblotting

Stimulated and un-stimulated cells were lysed as described (Marino et al., 1998). When indicated 1 μM ICI 182,780 or 10 μM U 0126 or 10 μM Ly 294002 or 5 μM SB 203580 were added to the medium 15 or 30 min, respectively, before agonist stimulation. Cells were solubilized in 0.125 M Tris-HCl (pH 6.8) containing 10% SDS (w/v), 1 mM phenylmethylsulfonyl fluoride, and 5 μg/ml leupeptin and boiled for 2 min. Proteins were quantified using the Bradford Protein Assay (Bradford, 1976). Twenty microgram solubilized proteins were resolved using SDS–PAGE at 100 V for 1 h. The proteins were then electrophoretically transferred to nitrocellulose for 45 min at 100 V at 4°C. The nitrocellulose was treated with 3% bovine serum albumin in 138 mM NaCl, 26.8 mM KCl, 25 mM Tris-HCl (pH 8.0), 0.05% Tween-20, 0.1% BSA, and then probed at 4°C overnight with either one of anti-ERα, anti-ERβ, anti-phospho-ERK, anti-phospho-AKT, anti-phospho-p38, anti-caspase-3, anti-Bcl-2, or anti-PARP antibodies. The nitrocellulose was stripped by Restore Western Blot Stripping Buffer (Pierce Chemical Company, Rockford, IL) for 10 min at room temperature and then probed with either anti-ERK, anti-AKT, or anti-p38 antibodies (1 μg/ml). Anti-actin antibody (1 μg/ml) was used to normalize the sample loading. Antibody reaction was visualized with chemiluminescence reagent for Western blot.

RESULTS

Divergent effects of E2 in inducing cell growth in the presence of ERα or ERβ

The level of exogenous ERα or ERβ was assessed in HeLa cells untrasfected (none) or transfected with either empty, ERα, or ERβ expression vectors. The Western blot analysis (Fig. 1a) confirmed the absence of ERs in both un-transfected and empty vector-transfected HeLa cells, whereas a unique band at 67 kDa (ERα-containing HeLa cells) or at 57 kDa (ERβ-containing HeLa cells) was detected. The time course of growth of HeLa cells transfected with empty plasmid or ERα or ERβ expression vectors was examined in the presence of E2 and in the presence of the ER inhibitor ICI 182,780. Figure 1b shows that the growth of empty plasmid-transfected HeLa cells was not affected by E2 or ICI 182,780 suggesting that the presence of ER is necessary for the hormone effects. On the other hand, E2 was mitogen for ERα-transiently transfected HeLa cells (Fig. 1c), whereas a decrease in growth was detected after E2 stimulation in ERβ-transfected HeLa cells with respect to unstimu-

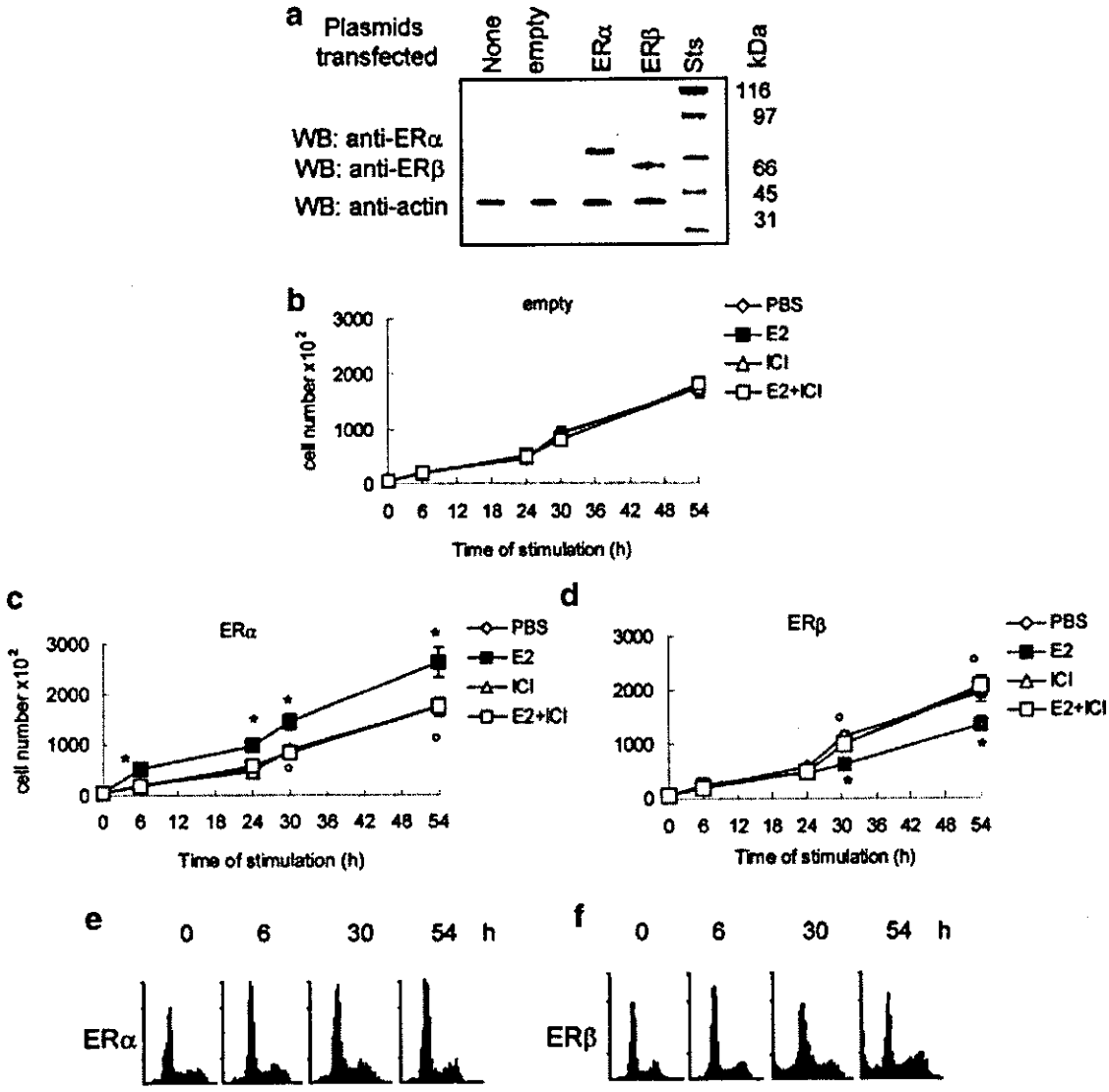

Fig. 1. Level of estrogen receptors (ERs) in transfected and un-transfected and time course of HeLa cell growth in the presence of 17β-estradiol (E2). Western blot analysis of ERα and ERβ levels were performed in un-transfected (none) or transfected HeLa cells with either empty, human ERα or human ERβ expression vectors (**part a**). HeLa cells transfected with empty (**part b**) or human ERα (**part c**) or human ERβ (**part d**) expression vectors were grown in DMEM in the presence of E2 (10 nM) and/or ICI 182,780 (ICI, 1 μM) counted at the indicated times. The data are the mean values ± SD of five independent experiments carried out in duplicate. $P < 0.001$, calculated with Student's t-test, compared with respective un-stimulated values (PBS) (*) or with E2-stimulated values (°). Flow cytometric analysis of the HeLa cells transfected with human ERα (**part e**) or human ERβ (**part f**) vectors after different time of E2-treatment compared with un-stimulated cells (0). The plots indicate cell cycle distribution present in sub-G1, G1, S, and G2/M phases, respectively. For details see the text.

lated ones (Fig. 1d). The cell pre-treatment with the ER inhibitor ICI 182,780 completely blocked the E2 effects both in ERα- and in ERβ-embedded HeLa cells. Further, we analyzed, by flow cytometry, the HeLa cell cycle distribution at different time after treatment. The typical plot of plasmid transfected-HeLa cell population is illustrated in Figure 1e and f (0 h). The first peak indicates the cell number in G1 phase of the cell cycle (50.0 ± 5.0%) followed by S phase (16.3 ± 3.2%), and by the peak of G2/M phase (19.8 ± 2.8%). Increasing the time of E2-stimulation (Fig. 1e; 6, 30, and 54 h), the number of cells in G1 phase of cell cycle increased reaching 65.4 ± 3.8% 54 h after the hormone administration to HeLa cells expressing ERα. On the contrary, when HeLa cells were endowed with ERβ (Fig. 1f; 6, 30, and 54 h), the number of cells in sub-G1 region increased reaching 9.5 ± 1.0% 54 h after the E2 stimulation thus suggesting the presence of DNA fragmentation.

Divergent effects of E2 in inducing an apoptotic cascade in the presence of ERα or ERβ

To determine whether the reported increase of cell population in the sub-G1 phase was truthfully related to the induction of an apoptotic cascade, we analyzed the cleavage of the caspase-3 proform (32-kDa band) which results in the production of the active subunit of the protease (17-kDa band). Caspase-3 proform was expressed in HeLa cells transfected with empty or ERα or ERβ expression vectors (Fig. 2a). No cleavage of caspase-3 was induced by E2 in empty or ERα-containing HeLa cells whereas E2 induced the production of the active subunit in the presence of ERβ.

To confirm that the appearance in the 17-kDa band was associated with an increase in caspase-3 activity, we analyzed one of the known substrates of caspase-3, PARP. This 116-kDa, DNA repair enzyme, is cleaved by

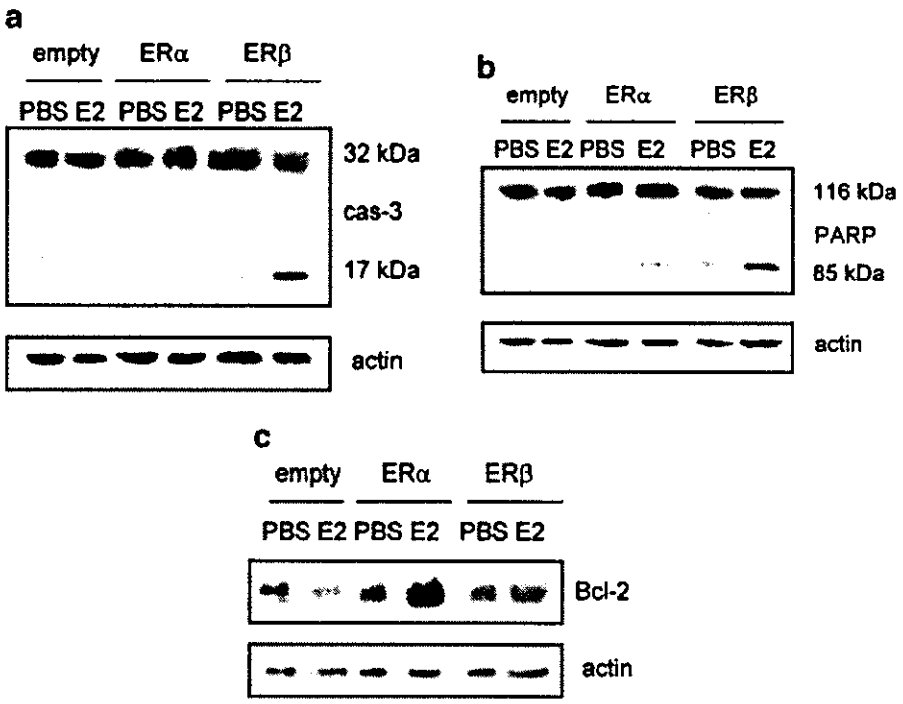

Fig. 2. Effect of E2 in the induction of pro-apoptotic proteins. Western blot analysis of caspase-3 (**part a**), PARP (**part b**) activation, and Bcl-2 (**part c**) levels were performed, as described in "Materials and Methods," on un-stimulated (PBS) and 24 h E2-treated (10 nM) HeLa cells transfected with human ERα, human ERβ, or empty expression vectors. The amounts of protein levels were normalized by comparison with actin expression. Typical blot of three independent experiments. For details see the text.

the caspase-3 producing the inactive 85-kDa fragment (Fig. 2b). By Western blot analysis, treatment of empty- and ERα-containing HeLa cells with E2 did not induce any conversion of PARP in the inactive form. On the contrary, the treatment of ERβ-transfected HeLa cells with E2 resulted in the conversion of PARP into the inactive 85-kDa fragment. These results were consistent with the idea that, in the presence of ERβ, E2 specifically induced an apoptotic cascade involving the caspase-3 activation and a downstream substrate like PARP. This was further confirmed by the expression of Bcl-2 level, the survival factor that can block both necrotic and apoptotic cell death (Dubal et al., 1999). Only the treatment of ERα-transfected HeLa cells with E2 markedly increased the amount of Bcl-2 (Fig. 2c).

Signal transduction pathways involved in the E2-induced apoptotic cascade

We previously reported that the rapid E2-induced activation of ERK/MAPK and PI3K/AKT pathways is sufficient and necessary for E2-induced cell cycle progression (i.e., DNA synthesis and the transcription of cyclin D_1 gene) (Marino et al., 2002, 2003). Then we asked if the inhibition of these rapid signals was involved in the E2–ERβ-induced apoptotic cascade.

No activation of signal transduction proteins was detected in cells transfected with empty vector and stimulated with E2 (data not shown). However, E2 increased ERK and AKT phosphorylation in HeLa cells transiently transfected with ERα (Fig. 3a). After reprobing the membranes using total ERK or AKT antibodies, to recognize the non-phosphorylated form of these proteins, the specific alteration of signaling proteins by E2 was confirmed to occur in the absence of changes in their expression levels (Fig. 3a). On the other hand, E2 failed to elicit any changes in the phosphorylation or expression level of ERK and AKT in cell expressing ERβ (Fig. 3a). Interestingly, a similar activation was observed in cancer cell lines which express endogenous ERα (HepG2) or ERβ (DLD1). In fact, E2 induced the rapid increase of ERK and AKT phosphorylation only in HepG2 cells (Fig. 3b) whereas it was ineffective in DLD1 cells (Fig. 3c). The level of endogenous ERα or ERβ was assessed in HepG2 and DLD1 cells. The Western blot analysis (Fig. 3d) confirmed the presence of a unique band at 67 kDa (HepG2 cells) or at 57 kDa (DLD1 cells) corresponding to ERα or ERβ, respectively.

Generally, the activation of PI3K/AKT and ERK/MAPK pathways causes cell survival in response to many mitogens and growth factors, whereas the activation of p38/MAPK has been associated with the regulation of apoptosis and differentiation processes (Ambrosino and Nebreda, 2001; Harper and LoGrasso, 2001; Talapatra and Thompson, 2001; Shimada et al., 2003; Porras et al., 2004). To verify this possibility, the effect of E2 on p38/MAPK activation was evaluated. A time course of E2-induced p38/MAPK phosphorylation in HeLa cells transfected with ERα or ERβ is shown in Figure 4a. A rapid and transient increase of p38/MAPK phosphorylation was detected from 15 to 30 min after E2 stimulation in ERα-transfected HeLa cells; whereas E2 induced a rapid (15 min) and persistent (24 h) increase of p38/MAPK phosphorylation in ERβ expressing HeLa cells. In the same way, E2 evoked a rapid (15 min) and transient activation of p38/MAPK in ERα-encoding HepG2 cells (Fig. 4b, upper part) and a rapid and persistent (24 h) phosphorylation of p38/MAPK in ERβ-containing DLD1 cells (Fig. 4b, lower part). Note that, the E2-induced p38/MAPK activation was prevented by the pure anti-ER ICI 182,780 in either cell lines (Fig. 4b). The same inhibitor completely